https://doi.org/10.57634/RCR5079

Single-atom catalysts in methane chemistry

Natalya V. Kolesnichenko, Natalya N. Ezhova,* Yulya M. Snatenkova

A.V.Topchiev Institute of Petrochemical Synthesis, Russian Academy of Sciences, Leninsky prosp. 29, 119991 Moscow, Russian Federation

The review integrates and systematizes literature data on the use of single-atom catalysts in methane chemistry, with the emphasis on the most recent results. The single-atom catalysts are heterogeneous catalysts of the latest generation in which single metal atoms supported on an inorganic material act as the active sites. The features of CH_4 activation on the surface of these catalysts are considered and compared with the behaviour of other known heterogeneous catalysts containing metal nanoclusters or active metal nanoparticles in relation to the direct oxidative and non-oxidative conversion of methane into various chemicals. The efficiency of application of single-atom catalysts of various compositions and types (supported single metal atoms, mono- and polymetallic monoatomic contacts, complex disperse compositions, *etc.*) is considered for reactions involving methane, including dry, steam and oxidative reforming, partial oxidation to methanol, oxidative carbonylation and carboxylation to acetic acid, non-oxidative and oxidative methane coupling to ethane/ethylene, methane dehydroaromatization, and methylation of benzene with methane. The new prospects opened up in methane chemistry by using single-atom catalysts are discussed.
The bibliography includes 307 references.

Contents

1. Introduction

Methane is the major component of natural gas and the most environmentally safe carbon resource for the production of high value-added chemical products.[1–7] Catalytic[1,2,8–14] and non-catalytic[15–22] methods for the conversion of this simplest hydrocarbon to basic products (hydrogen, ammonia, synthesis gas, ethylene, acetylene, carbon black and nanofibrous carbon, methanol, motor fuel, *etc.*) have been practiced for several decades; as a result, gas chemistry is now a leading branch of world economy with numerous large-scale plants (with a total capacity of >1 million tons per year) and a total production output of various chemicals of ~500 million tons per year.[16]

In recent years, the greatest attention of researchers has been directed towards development of processes for methane conversion to organic compounds that were previously commercially manufactured by petrochemical industry (oxygenates, olefins, aromatic hydrocarbons, polymers based on them, *etc.*).[3–7,11,12,23–36] There are two principal pathways for the conversion of gas feedstock to these products: indirect and direct conversion.[7,15,16,23–38] In the case of indirect conversion, CH_4 is converted to synthesis gas (CO and H_2 mixture), which is used for the industrial synthesis of oxygenates (methanol, dimethyl ether, acetic acid, methyl acetate) and other products.[18–20,29,39,40] In the case of direct methane conversion under oxidative or non-oxidative conditions, these valuable chemicals are obtained in one step.[4,6,21,36,37,41–46]

In view of the difficulty of activation of the thermally stable CH_4 molecule, until recently, the chemical reactions of methane were carried out only at high temperatures.[1,2,23,24] However, the high-temperature processes are energy demanding and expensive, and in the case of catalytic processes that enable conversion of methane under milder conditions, the use of harsh reaction conditions leads to a low stability of the catalyst structure and active sites and hampers selective preparation of target products (due to the higher reactivity of any other organic compound compared to CH_4).[2,3,6]

A variety of strategies have been attempted for decreasing the temperature of reactions involving methane.[47] Some research teams are developing methods for the conversion of methane under mild conditions in the presence of homogeneous catalytic systems.[31,48,49] However, the primary attention is devoted to the design of low-temperature (T = 25–300 °C) selective heterogeneous catalytic proc-

N.V.Kolesnichenko. Doctor of Chemical Sciences, Professor, Chief Researcher at TIPS RAS.
E-mail: nvk@ips.ac.ru
N.N.Ezhova. PhD in Chemistry, Leading Researcher at TIPS RAS.
E-mail: ezhova@ips.ac.ru; nnejova@mail.ru
Yu.M.Snatenkova. Junior Researcher at TIPS RAS.
E-mail: nvk@ips.ac.ru
Current research interests of the authors: nanoheterogeneous catalysis, single-atom catalysts, zeolite-based catalysts, gas chemistry, synthesis gas, methane, direct oxidative conversion of methane to oxygenates (acetic acid, methanol), methane conversion *via* synthesis gas and dimethyl ether to hydrocarbons (ethylene, propylene, petrol, aromatic compounds).

Translation: Z.P.Svitanko

Received 2 February 2022

© 2023 Uspekhi Khimii, ZIOC RAS, Russian Academy of Sciences

esses, which are most promising for the subsequent industrial implementation.[50] By analogy with known homogeneous catalysts, so-called quasi-homogeneous heterogeneous catalytic systems are developed.[51] Procedures of doping of traditional oxide catalysts have been used;[52, 53] transition metal alloys [54, 55] and proton-conducting oxide membranes with the perovskite structure [56, 57] have been proposed as catalysts. The most pronounced effect was attained on going to nano-sized catalytic systems.[23, 58–60] Meanwhile, special expectations of chemists are associated with the use of single-atom catalysts (SACs), which are able to activate methane even at room temperature.[61–64]

Single-atom catalysts are new-generation heterogeneous catalytic systems with monoatomic dispersion of metal active sites.[63, 65, 66] Unlike highly dispersed nano-sized systems (nanoparticles, nanoclusters), these systems have no metal–metal bonds on the surface. They are single metal sites (usually cations) that are chemically isolated and supported on an inorganic substrate.[67–70] All isolated metal atoms occur in direct chemical contact with the surface, which provides 100% accessibility for the reactants in chemical reactions. This configuration makes these heterogeneous catalysts somewhat similar to homogeneous catalysts [71, 72] and determines their unique properties: for most chemical reactions, SACs are effective under mild conditions and surpass in the activity, selectivity and stability other known heterogeneous catalytic systems, including those containing nanoparticles and nanoclusters of active metals.[73–78]

Single-atom catalysts differ from other catalytic systems in the electronic structure of the active sites.[71] It is not a single metal atom that is considered to be the SAC active site, but an active region centred by a single metal atom and including neighbouring atoms and/or vacancies.[63] These heterogeneous systems are characterized by strong interaction between the single metal site and chemical elements of the support (O, N, P, S *etc.*).[79] By varying the chemical composition of the support, it is possible to affect the electronic state of the active metal and to tune its catalytic properties.[79–81] The efficiency of a single-atom site is increased by using modification with organic ligands or doping with metals,[73, 75, 81–84] variation of the functional groups of the support,[66, 79] and, in some cases, special formation of complex dispersion systems that include, apart from isolated atoms, also nano or atomic clusters, or nanoparticles of active metals.[73, 81, 82]

Quite a number of single-atom catalysts have now been prepared; they contain a broad range of noble and some non-noble transition metal atoms [79, 85, 86] dispersed on supports of various chemical compositions and various natures.[82] The supports used for the formation of single metal active sites include metal oxides and sulfides,[87–90] metal and non-metal nitrides,[91–94] graphene (G) and graphite and their derivatives,[74, 76, 95, 96] porous structured materials like zeolites and metal-organic frameworks.[69, 97, 98] There are structurally diverse mono- and multimetallic heterogeneous contacts: catalysts with metal sites located on the support surface or embedded into the support crystalline framework [79, 85, 99, 100] or core@shell capsule catalysts.[74, 93–96] Nanostructured 2D systems (nanosheets, nanorods, *etc.*) have been obtained.[99, 101, 102] New types of SACs such as surface organometallic compounds [73, 103, 104] and single-atom metal alloys [105–107] have been synthesized.

Each type of single-atom heterogeneous catalysts has its own benefits. For example zeolites or metal-organic frameworks are used to obtain the most uniform catalytic structures.[97, 98] Nanostructured 2D systems are characterized by the maximum exposure of active sites and, hence, the highest production rate.[101] Single-atom alloys are distinguished by resistance to coking.[99, 107] Nano-heterogeneous systems of a complex size composition, in which synergistic effect occurs between single metal sites and other active species (atomic clusters or nanoparticles), exhibit unique catalytic properties in complex processes.[65, 76, 81, 108–110]

The rapid development of single-atom catalysis started in 2013–2014 [111] when new-generation high-resolution instrumental equipment was implemented in the research practice. It became possible to determine the catalyst fine structure at the atomic level using high-resolution transmission electron microscopy (HRTEM) and X-ray absorption spectroscopy (XAS) as extended X-ray absorption fine structure (EXAFS) or X-ray absorption near edge structure (XANES) techniques.[57, 66, 111] Particular research attention was attracted by the potential application of various types of SACs in redox reactions;[104] these catalysts have already showed high performance and high energy efficiency in a series of thermo-, electro- and photocatalytic processes [112–119] used in the production of organic compounds, energy engineering, environmental protection and biomedicine.[104, 120–122] However, the most impressive results were attained by the use of SACs in the chemistry of small molecules (CO, H_2, N_2, CO_2, CH_4),[65, 72, 78, 84, 123, 124] especially for the activation of strong chemical bonds (N≡N, O=C=O),[79, 96, 98, 110] including the C–H bonds of the thermally stable methane molecule.[72, 78, 84]

The studies dealing with SACs are rapidly developing, which is confirmed, in particular, by the apprarance of numerous reviews (>40);[63, 65–73, 77–79, 81–91, 97–107, 120–126] however, there are almost no studies specially devoted to the methane chemistry. There are only two review publications in international journals [125, 126] that summarize the results of studies of methane oxidation in the presence of single-atom catalysts and there are also particular chapters on similar topics in several more general reviews.[63, 72, 78, 103] Recent publications report the successful use of single-atom heterogeneous catalysts in other reactions in which methane is selectively converted to the target C_1 or C_{2+} products: dry, steam and oxidative reforming,[127–131] methylation,[132–135] oxidative carbonylation,[136–138] carboxylation [139–143] and oxidative [144] and non-oxidative [145–147] coupling. New publications on the application of SACs in methane chemistry continuously appear,[64, 147–150] but this rather extensive information has not yet been summarized.

This review analyzes, integrates and arranges the latest achievements in the application of SACs in the direct conversion of CH_4 to valuable chemical products (synthesis gas, C_1–C_2 oxygenates, C_{2+} hydrocarbons) both under oxidative and under non-oxidative conditions. New prospects for the catalytic transformations of methane in the presence of SACs caused by the specific features of CH_4 activation on single metal sites are demonstrated.

2. Features of methane activation by single-atom catalysts

The stable non-polar methane molecule is shaped like a regular tetrahedron and has a low polarizability and exceptionally high C–H bond dissociation energy ($\sim$439 kJ mol^{-1}). In most non-oxidative and oxidative

methane conversion reactions, dissociation of the first C–H bond in the CH_4 molecule is the rate-limiting step.[32]

Today, while developing low-temperature catalysts for reactions involving methane, chemists rely on the results of quantum chemical calculations,[151–153] which predict a markedly lower energy barrier for heterolytic dissociation of the methane C–H bond, *i.e.*, *via* polarization ($CH_4 \rightarrow :CH_3^{\delta-} + H^{\delta+}$), than for the homolytic dissociation to give radicals ($CH_4 \rightarrow {}^{\bullet}CH_3 + {}^{\bullet}H$). Therefore, preference is given to catalysts with charged active sites, which ensure the required polarization of the C–H bond.

The polarization of the CH_4 molecule is attained on solid catalytic surfaces containing Lewis pairs (acid and base), *e.g.*, on the Al_2O_3,[154,155] ZnO@Au,[156] boron nitride[157] and other surfaces. Heterolytic cleavage of the C–H bond is provided upon modification of zeolites or metal-organic frameworks with transition metal cations or oxide clusters.[158–164] Compounds considered to be promising for the heterolytic activation of methane include transition metal carbides and cationic boride clusters[59,165–168] and charged vanadium, manganese and rhenium oxide clusters.[169–171] Catalytic systems containing cationic heteronuclear oxide clusters ($[Al_2CuO_5]^+$, $[TiAlO_4]^+$, $[TiSiO_2]^+$) are also used.[130,131,172] The best results were achieved by using catalytic systems based on charged atomic clusters and ions (cations or anions) of noble and some non-noble transition metals: in the presence of these compounds, dissociation of methane molecule is possible even at room temperature.[59,61,149,173–184]

Using simplified models for transition metal cluster systems (M_n) in gaseous plasma, a number of researchers[176,177,182,185–200] demonstrated that the activity towards dehydrogenation of the methane molecule

$$CH_4 + M_n^{+(-)} \longrightarrow [H-M_n-CH_3]^{+(-)} \quad (1)$$

$$[H-M_n-CH_3]^{+(-)} \longrightarrow [M_nCH_2]^{+(-)} + H_2 \quad (2)$$

$$[M_nCH_2]^{+(-)} \longrightarrow [M_nC]^{+(-)} + H_2 \quad (3)$$

is inherent only in charged $M_n^{+(-)}$ clusters of moderate nuclearity ($n = 1–4$). When $n \geqslant 2$, the target process is, most often, accompanied by oligomerization of the $[M_nCH_2]^{+(-)}$ groups

$$[M_nCH_2]^{+(-)} + CH_4 \longrightarrow [M_nC_2H_4]^{+(-)} + H_2 \quad (4)$$

$$[M_nCH_2]^{+(-)} + CH_4 \longrightarrow [M_nC_2H_6]^{+(-)} \quad (5)$$

When $n = 1$, the process can be retarded after elimination of only one hydrogen atom from the methane molecule to give relatively stable methyl hydride complex [reaction (1)].[187,189,191] However, when a charged cluster with a complex chemical composition (*e.g.*, $[Rh_1Al_2O_4]^-$, $[Rh_1TiO_2]^-$)[183,184] contains a transition metal ion $M_1^{+(-)}$, the C–H bond in the methane molecule is cleaved *via* an alternative pathway, in which the methyl radical is attached to the noble metal atom site and the primary hydrogen atom is fixed on the heteroatom, *e.g.*, as shown below[184,201]

$$CH_4 + [Rh_1Al_2O_4]^- \longrightarrow [CH_3-Rh_1Al_2O_3OH]^- \quad (6)$$

The activity of these complex systems is several orders of magnitude higher than that of gas-phase transition metal ion.[176,183,184]

The model heteroatomic systems containing one active transition metal atom resemble real SACs in which the single-atom metal site (usually a cation) is supported on an inorganic material.[32,144,202] The electrophilic chemical elements (O, N, S, *etc.*) present on the support surface and bound directly to the active metal cation can participate in the activation of the primary C–H bond of methane by trapping the eliminated hydrogen atom. The hydrogen chemisorption on the polar sites of the support facilitates the C–H bond polarizability and increases the probability of its heterolytic cleavage with a reduced energy barrier. As a result, the temperature of methane activation decreases, and the methyl σ-complex $[CH_3-M_1]^+$ involving the active metal cation is formed.[203] According to the energy profile of methane dehydrogenation (Fig. 1 *a*), this complex has the lowest energy.[144] This attests to the high stability of this intermediate, which rules out the subsequent dehydrogenation steps. The formation of a stable methyl complex was detected by spectral methods for various SACs [Rh_1/ZrO_2,[144] Rh_1/CeO_2,[202] Pd_1/CeO_2,[203] H-Ta_1/SiO_2 (Ref. 204)] and the stability of such systems was confirmed by numerous quantum chemical calculations.[144,178,179,202,203]

Stabilization of the $[CH_3-M_1]^+$ methyl intermediate is a key feature of CH_4 activation by SACs, which determines their unique selectivity and the possibility of selective synthesis of organic products containing a methyl group (CH_3OH, C_2H_6, CH_3COOH, *etc.*) (Fig. 1 *b*). This feature accounts for the differences between the SAC behaviour in the methane chemistry and the behaviour of low-nuclearity atomic metal clusters, which form the basis of the modern nano-sized heterogeneous systems. Note that the latter catalysts show high activity towards the stepwise dissociation of the CH_4 molecule, which may result in complete dehydrogenation or be accompanied by oligomerization of the CH_2 or CH groups. These properties are valuable for catalysts meant for methane reforming processes (to give $CO + H_2$) or for CH_4 coupling processes giving a C_{2+} carbon skeleton. Catalytic systems with a complex size

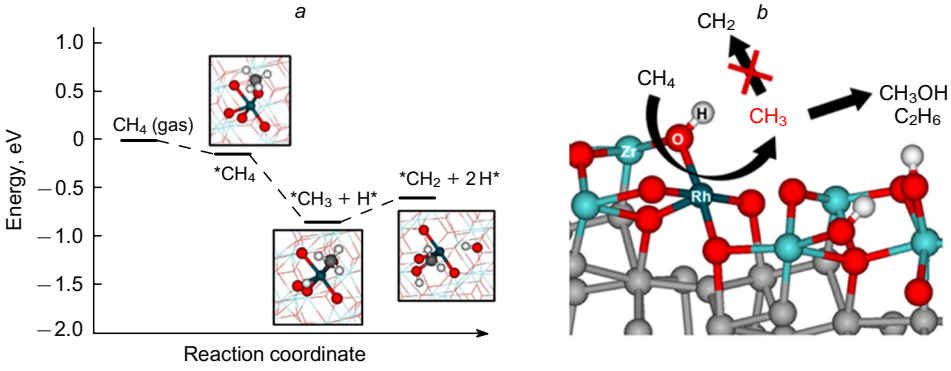

Figure 1. Energy profile of methane dehydrogenation over the $Rh_1^{3.6+}/ZrO_2$ single-atom catalyst (*a*) and CH_4 conversion pathways (*b*).[144] The asterisk refers to the excited state. Published with permission from the American Chemical Society (ACS).

composition containing simultaneously metal nanoclusters and single-atom metal sites may be of particular interest.

In the design of SACs, the choice of the support for the active site is an important factor, because adjustment of the strength of interaction between the metal cation and the support elements is a crucial aspect of tuning of the electronic state of the active site, which would influence its efficiency in the low-temperature methane conversion. For example, in the case of oxygen-containing supports (metal oxides, zeolites), the energy barrier for methane activation decreases with increasing negative charge on the substrate oxygen atom.[151] A similar situation was observed for the graphene support doped with nitrogen atoms.[205, 206] When zeolites are used as supports, the energy barrier for methane activation can be further reduced (by more than 50%) due to the synergistic effect caused by the presence of active metal ions in the catalyst and Brønsted acid sites in the zeolite framework.[158, 207]

Over the last ~5 years, >40 SACs based on noble (Rh, Pt, Pd) and some non-noble transition (Fe, Cu, Ni, Co, Zn, Cr, Ta, *etc.*) metal cations with various types of supports have been proposed for low-temperature methane activation (Table 1). The supports used for this purpose are mainly metal oxides with nanoparticle morphology (*e.g.*, nanowires, nanorods and so on) or zeolite matrices (usually in the H-form) with different crystal structures: MFI, CHA, MOR or BEA (items *2–23* in Table 1). Single active metal atoms can also be supported on monolayer single crystals (items *25*, *26*, *39*), fused with another metal (items *27–30*) or embedded into the graphene matrix (items *31–36*). Single-atom catalysts of unusual types have been designed. For example, there are single-atom alloys encapsulated into a silicate lattice or supported on metal oxide nanoparticles (items *29*, *30*). A more intricate system has also been proposed, that is, graphene matrix with attached single rhodium atoms, which are bound by strong covalent bonds to nickel single crystals (item *39*). Molybdenum sulfide and porous carbon nitride, including its oligomeric polymorphs (items *37*, *38*, *40*) are also considered as promising supports. Hexagonal boron nitride sheets possessing high thermal conductivity (item *41*) are considered to hold good promise as a support material for single-atom catalysts.

The efficiency in the activation of methane molecules for most of the proposed SACs has so far been investigated by theoretical computer simulation methods (mainly DFT). Some of these catalysts have already been tested in kinetic experiments in various oxidative and non-oxidative methane conversion reactions.

3. Reforming of methane into synthesis gas

Methane reforming is one of the few modern large-scale industrial processes for the oxidative processing of natural gas for the formation of synthesis gas.[39, 246–248] This gas mixture is used as a source of hydrogen for the production of ammonia and mineral nitrogen fertilizers[247] and as an intermediate in large-scale industrial processes such as synthesis of methanol,[249, 250] acetic acid,[24] formaldehyde, ethers,[251] lower olefins [23] and synthetic fuel.[252]

The existing commercial processes of methane conversion to synthesis gas involving the use of oxidants (H_2O, O_2, CO_2) at high temperatures (800–950 °C) catalyzed by heterogeneous nickel-containing oxide cermets[253–255] are characterized by high energy consumption and fast catalyst deactivation, mainly as a result of carbon deposition on the catalyst surface.[246, 256]

The hope for efficient elimination of the drawbacks of the industrial methane reforming processes is placed, in particular, on the replacement of the traditional heterogeneous bulk catalysts by single-atom catalytic systems:[68, 216] owing to the low-energy heterolytic cleavage of the primary C–H bond upon CH_4 activation on SAC active sites, it is possible to decrease the reaction temperature, while stabilization of the methyl intermediate prevents methane pyrolysis and oligomerization, which are the major causes of coking and carbonization of the catalytic surface.

According to the results of quantum chemical calculations,[68, 216, 217] the CH_4 conversion to $CO + H_2$ over SACs consists of a sequence of reactions of the methyl intermediate including oxidative dehydrogenation steps

$$*CH_3 \longrightarrow CH_3O* \longrightarrow CH_2O* \longrightarrow CO \qquad (7)$$

This process is chemically complex and requires catalysts of definite chemical and phase compositions.

In a number of studies,[181, 183, 184] mass spectrometry and photoelectron spectroscopy were used to study the behaviour of rhodium-containing anionic species of two types, those doped with one noble metal atom ($[Rh_1Al_2O_4]^-$, $[Rh_1TiO_2]^-$)[183, 184] and those consisting of three rhodium atoms (Rh_3^-),[181] in the methane reactions with oxidants (O_2, CO_2) proceeding under ideal thermal collision conditions (at temperatures close to room temperature). In relation to these models it was shown that single-atom systems can promote and low-nuclearity atomic clusters can catalyze the conversion of methane to synthesis gas under thermal conditions. In view of this, researchers attempt to use SACs in methane reforming both separately and as parts of complex dispersed catalytic systems containing single atoms of the active metal together with low-nuclearity nanoclusters (Table 2).

Most of the known single-atom heterogeneous catalysts for methane reforming are based on nickel or noble metals (Ru, Pt, Rh) supported on various materials.[127–131, 216, 217, 222, 257] Using wet impregnation[131, 222, 257] or strong electrostatic adsorption,[128, 216] the single-atom sites of active metals are introduced, in the form of cations, into zeolite matrices (MOR, BEA, MFI),[222] cerium oxide[217] or hydroxyapatite lattice.[128, 131, 216] Atomically dispersed systems with strong bonds between the metal and the support can also be obtained by combustion of nitrogen-containing metal precursors mixed with the oxide support (lanthanum oxide). Apart from active metals, doping components such as calcium oxide,[131] cobalt oxide[222] or lanthanide oxides (CeO_2, Sm_2O_3) are added to the catalysts.[216, 257] In all cases, during the catalyst formation, chemical elements of the support or the doping promoter [Brønsted acid sites (BAS), Ca^{2+}, Ce^{4+} cations and so on] are partially replaced by cations of the active metal ($M^{\delta+}$). This gives rise to a new interfacial structure (such as $M^{\delta+}-O-Al$,[222] $M^{\delta+}-O-P$,[128] $M^{\delta+}-O-Ce$[216, 217]), which provides stability of the single-atom site capable of activating methane by the low-energy-consuming heterolytic mechanism, in which the hydrogen atom eliminated upon dissociation of the methane C–H bond can be chemisorbed on an oxygen atom of the support.

Apart from the conventional supported SACs, more complex heterogeneous catalysts have also been proposed for methane reforming, particularly, polymetallic single-

Table 1. Single-atom catalysts for methane activation under non-oxidative and oxidative conditions.

No.	Catalyst	Charged active site	Activation conditions		Investigation method	Ref.
			T, °C	oxidant		
1	Pt_1^- (anionic cluster)	Pt^-	–	None	DFT	187
				CO_2	DFT	188
2	M_1/TiO_2 (111) (nanoparticles)	–	< 25	None	DFT	179, 208
	(M = Pt, Pd, Rh, Os, Ir)					
3	Cr_1/TiO_2 (nanoparticles)	–	50	H_2O_2	KE	209
4	Pt_1/TiO_2 , Pt_1/GeO_2	Pt^+	–	None	DFT	210
5	$Pt_1/SrTiO_3$ (100)	Pt^-	–	None	DFT	211
6	Rh_1/TiO_2 (nanoparticles)	–	150	O_2 + CO	KE	212
7	Rh_1/ZrO_2	$Rh^{3.6+}$	50	H_2O_2	DFT, KE	144, 213, 214
		$Rh^{3.6+}$	260	O_2	DFT, KE	144
8	Rh_1/CeO_2 (nanowire)	$Rh^{\delta+}$	50	H_2O_2	DFT, KE	202
9	Pt_1/CeO_2 (111) (nanoparticles)	–	25	CO_2	P-C	180
10	Pt_1/CeO_2 , Ni_1/CeO_2 , Co_1/CeO_2	–	25	None	DFT, P-C	178
11	Ag_1/CeO_2	Ag^+	–	None	DFT	215
12	Ni_1-CeO_2/HAP	–	500	CO_2	KE	216
13	Ni_1-Ru_1/CeO_2 (nanorods)	–	560	CO_2	KE	217
14	Zn_1-CeO_2 , Zn_1-CeO_2/MMT	Zn^{2+}	300	CO_2	DFT, KE	139, 218
15	Rh_1/H-ZSM-5 (H-MFI)	$Rh^{\delta+}$	150	O_2 + CO	DFT, KE	136, 219
16	Rh_1/H-CHA (H-SSZ-13)	$Rh^{\delta+}$	150	O_2 + CO	KE	220, 221
17	Rh_1-Co/H-MOR	$Rh^{\delta+}$	650	O_2	KE	222
18	$CuO-Pd_1$@H-ZSM-5	–	95	H_2O_2	KE	223
19	Cu_1/H-ZSM-5 (H-MFI)	–	50	H_2O_2	P-C, KE	150, 224
20	Cu_1/H-CHA (H-SSZ-13)	–	200	O_2 + CO	KE	137, 220
21	Fe_1/H-ZSM-5 (H-MFI)	$Fe^{\delta+}$	50	H_2O_2	DFT, KE	225, 226
22	Zn_1/H-ZSM-5, Zn_1/H-MOR	Zn^{2+}	300	CO_2	KE	139
		Zn^{2+}	300	CO_2	P-C	227
		Zn^{2+}	300	O_2	P-C	229
		Zn^{2+}	25	None	P-C	228, 230, 233
		Zn^{2+}	25	None	DFT	228, 231
				CO_2	DFT	231, 232
23	Zn_1/H-BEA (H-β)	Zn^{2+}	25	None	DFT	234
24	H-$Ta_1(SiO)_2$	–	250	None	KE	235
25	Pd_1/Cu (111)	–	–	O_2	DFT	236
26	M_1/Cu (111) (M = Ru, Rh, Co)	–	–	None	DFT	237
27	Pd_1Au (alloy)	–	–	None	DFT	208
28	Pt_1Cu (alloy), Pt_1Ni (alloy)	–	–	None	DFT	238
		–	–	O_2		236
29	Pt_1NiCe (alloy) @SiO_2	–	500	CO_2	KE	127
30	Co_1Ni (alloy)/CeO_2	–	600	CO_2	KE	239
31	Al_1@G, Ga_1@G, Co_1@G	–	–	N_2O	DFT	240, 241
32	Co_1@G, Ni_1@G	–	–	None	DFT	242
33	Cu_1@G, Zn_1@G	–	–	O_2	DFT	206
34	$Zn_1@N_2C-G$, $Zn_1@N_3-G$	–	–	O_2	DFT	206
35	$Fe_1@N_3-G$	–	25	None	DFT	205
		–	–	H_2O_2		149
36	$Fe_1@N_4-G$	–	25	H_2O_2	P-C	61
37	Cu_1/C_3N_4	–	25	H_2O_2	KE	205
38	$Ti_1@C_{24}N_{24}$, $V_1@C_{24}N_{24}$	–	–	N_2O	DFT	243
39	Rh_1@G/Ni (111) (nanoparticles)	–	200	O_2	DFT	244
40	$Fe_1@Mo_6S_8$	–	–	H_2O	DFT	245
41	M_1/BN (M is transition metal)	–	–	O_2	DFT	92

Note. The following abbreviations and symbols are used: DFT is density functional theory; KE is kinetic experiment; P-C are physicochemical methods; HAP is hydroxyapatite, hexagonal phosphate, $Ca_{10}(PO_4)_6(OH)_2$; MMT is montmorillonite, a layered clay mineral with a great surface area, $(Na,Ca)_{0.33}(Al,Mg)_2(Si_4O_{10})(OH)_2 \cdot n\,H_2O$; MFI is mordenite framework inverted, $Na_xAl_xSi_{96-x}O_{192} \cdot 16\,H_2O$, $0 < x < 27$; ZSM-5 is Zeolite Socony Mobil-5 with the MFI structure; CHA is chabazite structure, $Q_xNa_yAl_{2.4}Si_{33.6}O_{72} \cdot z\,H_2O$, Q is *N*,*N*,*N*-1-trimethyladamantammonium, $1.4 < x < 27$, $0.7 < y < 4.3$, $1 < z < 7$; SSZ-13 is high-silica aluminosilicate zeolite material with CHA structure corresponding to the ABC-6 zeolite family; MOR is mordenite, $(Ca,Na_2,K_2)[Al_2Si_{10}O_{24} \cdot 7\,H_2O]$; BEA is β-zeolite, $Na_7Al_7Si_{57}O_{128}$. The zeolite names are given in accordance with the international classification published in Ch.Baerlocher, L.B.McCusker, D.H.Olson. *Atlas of Zeolite Framework Types*. (6th Edn) (Elsevier, 2007); elsevier.com/books/atlas-of-zeolite-framework-types/baerlocher/978-0-444-53064-6.

Table 2. Methane reforming to synthesis gas over single-atom catalysts.

No	Catalyst	T, °C	CH_4 conversion (%)		Selectivity (%)		Specific reaction rate[a] (mmol CH_4) g_{cat}^{-1} h^{-1}	TOF,[b] s^{-1}	Ref.
			1 h	⩾10 h	H_2	CO			
				Dry (carbon dioxide) reforming of methane					
1	Ni_1/HAP	750	80	76	–	–	4085	13	128
2	Ni_1/Ce-HAP	750	95	95	–	–	1865	6	216
3	Ni_1/Ca-HAP (nanorods)	600	–	–	–	–	122	–	131
4	Ni_1/CeO_2 (nanorods)	600	63	–	80	–	–	35	217
5	Ru_1/CeO_2 (nanorods)	600	83	–	83	–	–	55	217
6	Ni_1-Ru_1/CeO_2 (nanorods)	560–600	91	90	98.5	–	–	74	217
7	$Pt_1-NiCe@SiO_2$	500	5	6	–	–	76	–	127
8	$Pt_1-NiCe@SiO_2$	750	73.5	64.5	99	–	–	–	127
				Steam reforming of methane					
9	$Rh_1/Sm_2O_3-CeO_2-Al_2O_3$	500	–	–	–	–	302	1.8	257
10	$Rh_1-Rh_n/CeO_2-Al_2O_3$	500	–	–	–	–	440	2.3	257
				Partial oxidation of methane					
11	Rh_1@H-MOR	600	6	6	–	39	–	–	222
12	Rh_1-Co_n/H-MOR	600	15	15	–	90	–	–	222
13	Rh_1-Co_n/H-MOR	650	85–86	85–86	–	91	1262	72	222

[a] After 10 h of catalyst operation; [b] TOF is the turnover frequency of the single-atom metal active site per unit time (after 0.5–1 h of catalyst operation).

atom systems (Ni_1-Ru_1/CeO_2,[217] Rh_1-Co/H-MOR [222]), single-atom alloys (Pt_1-NiCe),[127] encapsulated systems ($Pt_1-NiCe@SiO_2$),[127] and systems of a mixed size composition, including simultaneously single-atom metal sites and metal nanoclusters ($Rh_1-Rh_n/CeO_2-Al_2O_3$,[257] Rh_1-Co_n/H-MOR [222]).

The efficiency of a particular catalyst design depends, first of all, on the oxidant (CO_2, H_2O or O_2) used for CH_4 conversion (see Table 2). However, in all cases, in the design of SACs for methane reforming, chemists have followed the strategy according to which CH_4 and the oxidant are activated on different sites.

Single-atom catalysts for dry reforming (CO_2 as the oxidant) are often bimetallic systems that comprise a single-atom metal site (Ni, Pt, Ru) where the CH_4 molecules are activated and a basic site meant for the adsorption and dissociation of CO_2 molecules (cerium oxide,[217] calcium oxide,[131] *etc.*). The synergistic effect caused by the presence of two sites for reactant activation is most pronounced in the case of the polymetallic catalyst with two heterometallic single-atom sites (nickel and ruthenium) that are directly bound to each other and are fixed on cerium oxide nanorods (Ni_1-Ru_1/CeO_2).[217] According to Tang *et al.*,[217] the primary C–H bond of the CH_4 molecule dissociates on the nickel site, and the resulting H atoms migrate to ruthenium (hydrogen spillover) where they are converted to molecular hydrogen. The CO_2 molecule is adsorbed on the ruthenium atom, and its dissociation takes place with participation of cerium oxide defects

$$CO_2 \longrightarrow CO + O \quad (8)$$

Thus, all components of the Ni_1-Ru_1/CeO_2 catalytic composition, including the support, are involved in the reactant activation and CO and H_2 formation.

A catalytic system effective for steam reforming of methane (with H_2O as the oxidant) has a mixed size composition, including single-atom Rh_1 sites and Rh_n nanoclusters supported on cerium oxide-doped alumina ($Rh_1-Rh_n/CeO_2-Al_2O_3$).[257] In the opinion of Duarte *et al.*,[257] methane activation takes place on rhodium single-atom sites, but they are inert towards water molecules; the H_2O activation and CO formation occur on rhodium nanoclusters. The activation of water molecules involves both Rh_n nanoclusters and CeO_{2-x} promoter: the oxygen atoms formed on the rhodium sites migrate to CeO_{2-x} vacancies *via* spillover. Thus, methane conversion to synthesis gas upon the reaction with water is provided by the synergistic effect of three components of the complex catalytic system: Rh_1, Rh_n and CeO_{2-x}.

Different-size catalysts with a single-atom site and a metal nanocluster formed by different metals are also used for the partial oxidation of methane to synthesis gas (oxidative reforming, O_2 as the oxidant). For example, the Rh_1-Co_n/H-MOR bimetallic system has been proposed;[222] in the authors opinion, methane molecules are activated on the single-atom rhodium site, while oxygen molecules are mainly activated on the cobalt nanoclusters. Cobalt is oxidized during the process, but is rapidly reduced to Co^0 under the action of hydrogen, which results from methane dissociation on Rh_1 site and migrates towards cobalt *via* spillover. The metallic components of this catalytic system were fixed in the zeolite matrix, which is not involved in the reforming of methane, but maintains the highly dispersed state of the active metal sites.[257, 258]

The catalytic properties of single-atom systems towards methane reforming have been compared with the properties of heterogeneous catalysts of the same composition, but fully consisting of metal nanoclusters.[127, 128, 216, 257] The following pairs of systems were tested in the dry reforming of methane: Ni_1/Ce-HAP and Ni_n/Ce-HAP,[216] $Pt_1-NiCe@SiO_2$ and $Pt_n-NiCe@SiO_2$ [127] and Ni_1/HAP and Ni_n/HAP;[128] also, Rh_1/Al_2O_3 and Rh_n/Al_2O_3 were tested in the steam reforming.[257] According to the results, at any type of reforming, the starting activity was 2.5–4

times higher for single-atom systems than for nanoclusters, all other factors being equal. The catalytic properties of single-atom systems were virtually invariable for at least 50–100 h,[216, 222] whereas nanoclusters were rapidly coked and deactivated in the first 10–15 h.[256] The above cited authors obtained experimental data, demonstrating advantages of single-atom catalysts over nanocluster systems such as higher starting activity, the possibility of reducing the reaction temperature down to 500–750 °C, resistance to coke formation and increase in the time of continuous operation of the catalyst before regeneration.

Apart from the single-atom metal active sites, the surface of SACs may carry metal nanoclusters of different size and nanoparticles (Fig. 2 *a*). Akri *et al.*,[216] who investigated dry reforming of methane on heterogeneous Ni_1/Ce-HAP and Ni_n/Ce-HAP catalysts, showed that a heterogeneous catalyst composed of nanoclusters and a large amount of nanoparticles (10% Ni_n/Ce-HAP) is rapidly deactivated during the reforming, but the presence of a small amount of nanoclusters in the single-atom catalyst has a beneficial effect on the catalyst performance [activity and resistance to coking, *cf.* 0.5% Ni_1/Ce-HAP and 2% (Ni_1-Ni_n)/Ce-HAP in Fig. 2 *b*,*c*].

A number of highly active and stable catalytic compositions with single-atom metal sites suitable for the industrial implementation have been proposed to date. For example, the Rh_1-Co_n/H-MOR system was developed for partial oxidation of methane to synthesis gas ($H_2:CO = 2$ molar ratio) at 650 °C,[222] while the Ni_1-Ru_1/CeO_2 system was designed for dry reforming at temperatures of 560–600 °C;[217] in particular, it was tested in fuel cells at 500 °C.[259] In the presence of these catalytic compositions, reforming proceeds with a selectivity of 90–99% (to CO and H_2), with methane conversion being 85–90%. On each catalytic active site, 72–74 H_2 molecules per second are formed without noticeable coke formation.

The studies on the development of SACs for methane reforming are still few in number, but the obtained results already attest to high potential of these innovative catalytic systems in industry with the possibility of reducing the reaction temperature by 200–250 °C and considerable increase in the operating time of the catalyst.

4. Direct oxidative conversion of methane into oxygenates

The prospects of direct one-step conversion of methane to oxygenates has long attracted the attention of a broad range of researchers [3, 4, 25, 48, 260, 261] as a possibility of decreasing the number of stages in the advanced industrial processing of natural gas. In recent years, the probability of practical solution of this problem has markedly increased owing to the targeted development of SACs for these reactions.

In view of the ability of these catalysts to stabilize the methyl intermediate upon the methane activation, chemists make attempts to prepare effective single-atom heterogeneous catalysts for the direct oxidative conversion of methane to organic compounds containing a CH_3 group, that is, methanol and acetic acid, which are large-scale industrial products.[125, 126, 138, 262, 263]

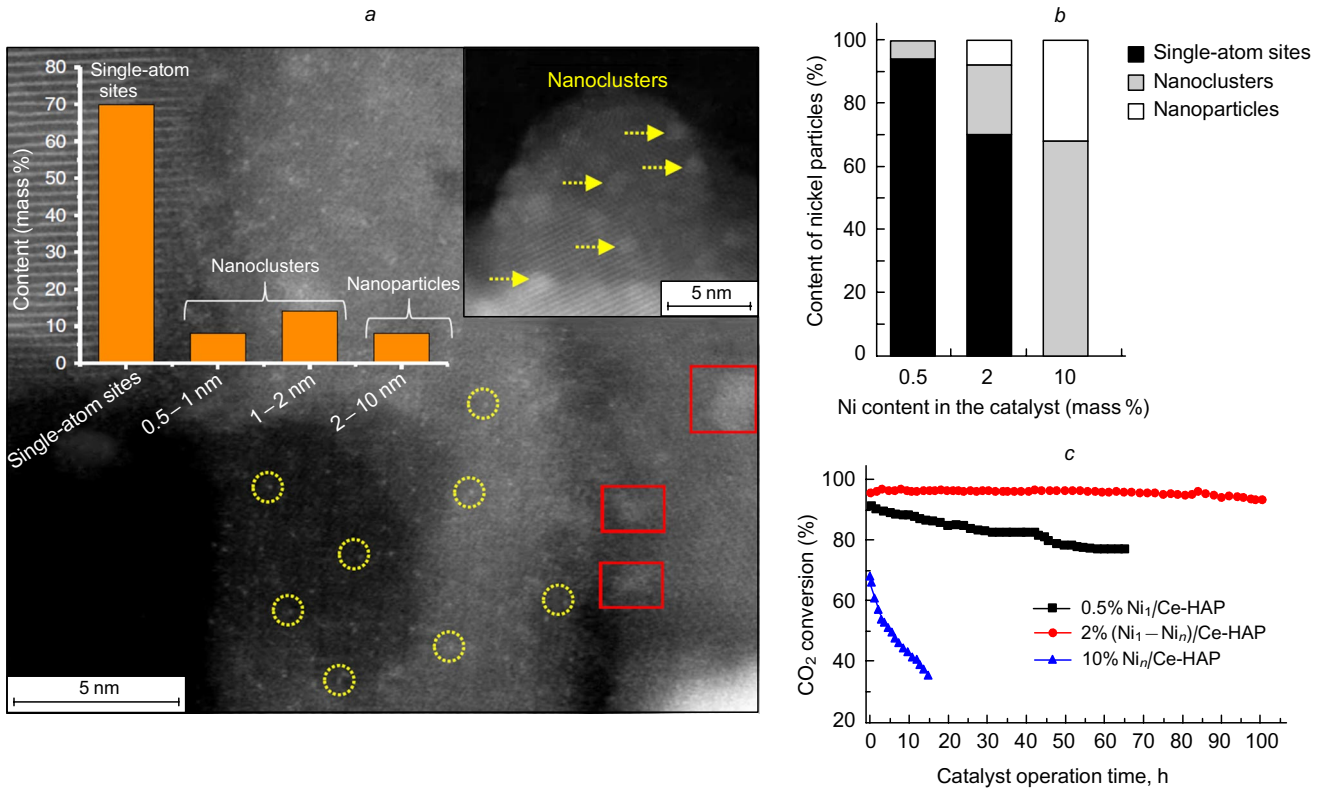

Figure 2. HRTEM images of the 2% (Ni_1-Ni_n)/Ce-HAP sample (the circles mark single-atom sites and the squares mark nanoclusters) and distribution diagram of nickel-containing particles of various sizes on its surface (*a*); distribution of nickel single-atom sites, nanoclusters and nanoparticles on the surface of Ni/Ce-HAP catalyst with Ni content of 0.5, 2 and 10 mass % Ni (*b*) and CO_2 conversion in methane dry reforming over these catalysts (reaction conditions: $T = 750$ °C, $CH_4:CO_2:He = 10:10:30$, gas flow rate 50 mL min^{-1} (60 000 mL $g_{cat}^{-1} h^{-1}$) (*c*).[216] Published under the Creative Commons Attribution 4.0 International License.

Examples of SACs experimentally studied by various research groups in the direct methane oxidation to oxygenates with various oxidants such as hydrogen peroxide,[223, 262] oxygen and carbon monoxide mixture [138, 212, 263] and carbon dioxide [139] are summarized in Table 3. The Table includes mono- and polymetallic heterogeneous catalysts with single-atom sites of noble metals, Rh,[136, 144, 202, 263] Pd,[138, 223] Ir,[138] and systems based on some non-noble metals: Fe,[61, 64, 148, 226] Cu,[137, 150, 264] Cr,[209] Zn,[139] Ni.[262] The supports used in these systems are metal oxides [TiO_2,[190] ZrO_2,[144] CeO_2 (Ref. 202)], zeolites (H-ZSM-5,[64, 150, 223] H-MOR [148] or H-SSZ-13 [137]) and carbon materials usually functionalized with nitrogen (nitrogen-containing graphene [149] and carbon nanotubes,[262] porous carbon nitride [264]).

It can be seen from Table 3 that the oxidative conversion of methane in the presence of SACs is a low-temperature process selective to CH_3-containing oxygenates, the proportion of which in the product reaches 70–100%. In the methane oxidation with hydrogen peroxide, high selectivity to methanol is attained in some cases (see Tables 3, items *1–11*); the reaction of CH_4 with CO_2 gives acetic acid (item *21*) or acetic and formic acids (item *20*), and the reaction of methane with oxygen in the presence of carbon monoxide may afford methanol and acetic and formic acids (items *12–19*). Irrespective of the oxidant used, almost no deep oxidation products (CO_2, CO) are formed in the presence of single-atom catalytic sites. However, when methane reacts with H_2O_2, the products can also contain organic peroxides (methyl peroxide, hydroxymethylene peroxide). Currently, the efforts of chemists are directed towards increasing the selectivity to the target oxygenate products.

Most studies are devoted to the development of SACs for the selective methane oxidation to methanol with hydrogen peroxide. This reaction occurs under the mildest conditions: at $T = 25–95$ °C in water (see Table 3, items *1–11*). Recent studies [61, 144, 149, 202, 262, 264] demonstrated that the formation of formic acid in this oxidative reaction can be minimized when the single-atom sites of active metal (Rh, Fe, Cu, Ni) are immobilized on nitrogen-doped carbon supports or attached to the surface of some metal oxides (ZrO_2, CeO_2). This result is attributable to the synergistic effect of the support and the active metal in the reactant activation.[61, 144, 149, 209] The support participates in the adsorption and spontaneous dissociation of hydrogen peroxide [61, 144, 213]

$$H_2O_2 \longrightarrow H_2O + {}^{\bullet}O \quad (9)$$

$$H_2O_2 \longrightarrow {}^{\bullet}H + {}^{\bullet}OOH + {}^{\bullet}OH \quad (10)$$

The resulting radicals are attached to the support surface, which prevents the excess oxidation of reactants. The adsorbed highly reactive $^{\bullet}OOH$ (Ref. 144) or $^{\bullet}O$ (Ref. 61) radicals react with the active metal atoms to give metal-oxo sites, which are highly active in the dissociation of the primary C–H bond of methane to give the $^{\bullet}CH_3$ radical, which recombines with the $^{\bullet}OH$ and $^{\bullet}OOH$ radicals, giving rise to methanol (CH_3OH) and its precursor, methyl peroxide (CH_3OOH).[213, 265] Owing to stabilization of the $^{\bullet}CH_3$ radical, the reaction selectivity to methyl-containing products ($CH_3OH + CH_3OOH$) exceeds 95%. However, methyl peroxide may dominate in the products over methanol, as a result of the general retardation of the process. It is believed [225] that in the single-atom catalytic systems with an active support, the reactants (H_2O_2 and CH_4) can compete for the same active sites; since H_2O_2 dissociation is energetically more favourable than the homolytic cleavage of the primary C–H bond of CH_4 and its oxo functionalization, the overall efficiency of the methane oxidation remains low: the turnover frequency of the metal active sites per unit time is 0.5–27 h^{-1} (see Table 3, items *1–6*).

A much higher (10–1000-fold) activity is inherent in SACs obtained by immobilization of active metals in micropores of a zeolite matrix [Cu_1@H-ZSM-5,[150] Fe_1@H-ZSM-5,[226] Fe_1–CuO/H-ZSM-5,[64] Pd_1@H-ZSM-5 [223] and Pd_1–CuO/H-ZSM-5 (see Ref. 223 and Table 3, items *7–11*)]. The exceptionally high activity of these systems is attributed to the high content of the cationic species of the active metal (Pd^{2+}, Cu^{2+}, Fe^{2+}) located in the channels of a structured microcrystalline material;[64, 223] this creates conditions for the heterolytic cleavage of the C–H bond, which is more energy efficient than the homolytic dissociation of this bond. In these catalysts, the zeolite support does not participate in H_2O_2 activation and cannot scavenge radicals (which are inevitably generated in any oxidative process involving H_2O_2); therefore, the reaction in the presence of these catalysts affords a large amount of excessive oxidation products such as formic acid and methyl peroxide, the proportion of which can reach 93% (see Table 3, items *7*, *10*). In order to suppress the formation of these products, copper(II) oxide is added to the catalytic system as a radical scavenger.[266, 267] This results in the formation of a bimetallic catalyst selective to methanol (78–80%) [Fe_1–CuO/H-ZSM-5,[64] Pd_1–CuO/H-ZSM-5 (see Ref. 223 and Table 3, items *9*, *11*)].

A high methanol selectivity (79%) was found for the monometallic copper single-atom catalyst Cu_1@H-ZSM-5.[150] Palladium doping of copper oxide deposited on the H-ZSM-5 zeolite surface (the noble metal content being at the impurity level, only 0.01 mass %) gave the most active catalyst — 0.01% Pd_1–CuO/H-ZSM-5 (see Table 3, item *11*). With this bimetallic system, the synthesis of methanol is carried out at 50 °C with a production rate of ~4 mol kg_{cat}^{-1} h^{-1} at a selectivity of 78%. When the reaction temperature is increased to 95 °C, the rate of formation of the target product can be doubled (up to ~8 mol $kg_{cat}^{-1}h^{-1}$) and the selectivity increases up to 86%, while the formation of the side oxygen-containing products (HCOOH and CH_3OOH) is almost suppressed.

A review [78] and several papers [144, 202, 264, 268] reported comparison of the reactions between CH_4 and H_2O_2 in the presence of single-atom catalysts and nanocluster systems of the same composition: Rh_1@ZrO_2 and Rh_n/ZrO_2,[144] Rh_1@CeO_2 and Rh_n/CeO_2,[202] Cu_1@C_3N_4 and Cu_n/C_3N_4,[264] and Fe_1@H-ZSM-5 and Fe_n/H-ZSM-5.[226, 268] All authors noted pronounced increase in the reaction rate (5–8-fold) and selectivity to methanol (1.5–3-fold) on going from the nanoclusters to SACs. On the basis of the results of kinetic experiments and calculations, various reaction pathways for methane conversion, resulting in different products, were proposed. For example, as can be seen from the energy profiles of product formation during methane oxidation with hydrogen peroxide in the presence of Rh_1@CeO_2 and Rh_n/CeO_2 systems (Fig. 3), the energetically favourable pathway in the case of single-atom sites includes dissociation of the primary C–H bond of the methane molecule to give the $^{\bullet}CH_3$ methyl intermediate

Table 3. Direct oxidative conversion of methane to oxygenates over single-atom catalysts.

No.	Catalyst	Reaction conditions		TOF, h^{-1}	Specific rate of oxygenate formation, (mmol of the product) $g_{cat}^{-1}\ h^{-1}$				Selectivity (%)			Ref.
		T, °C	P_{CH_4}, MPa		CH_3OH	CH_3COOH	HCOOH	CH_3OOH	CH_3OH	CH_3COOH	CO_2	
	Oxidant: H_2O_2, liquid-phase heterogeneously catalyzed reaction, aqueous medium											
1	2.7% Fe_1@N–G	25	2	0.5	0.009	0	0.012	0.215 [a]	4	0	6	61, 149
2	1% $Cu_1@C_3N_4$		3	~1	0.193	0	0	0.867	~17	0	~6	264
3	0.7% Ni_1@N–CNT	50	2	9	1.010	0	0	0.053	95	0	0	262
4	0.5% Cr_1/TiO_2		3	3	0.380	0	0.150	3.990 [a]	53	0	0	209
5	0.5% Rh_1/CeO_2 (nanowire)		0.5–1	27	1.000	0	0	0.280	76	0	2	202
6	0.3% Rh_1/ZrO_2	70	3	~2	0.036	0	0	0.002	71	0	20	144
7	0.34% Cu_1@H-ZSM-5	50	3	179	7.680	0	1.200	0.864 [a]	79	0	1	150
		70	3	448	12.000	0	9.600	1.800 [a]	50	0	3	150
8	0.1% Fe_1@H-ZSM-5	25	2	367	0.059	0	0.145	0.146 [a]	16	0	3	226
9	0.1% Fe_1–CuO/H-ZSM-5	25	2	539	0.385	0	0	0.084 [a]	80	0	3	64
10	0.01% Pd_1@H-ZSM-5	50	3	8820	0.528	0	4.344	2.820	7	0	4	223
11	0.01% Pd_1–CuO/H-ZSM-5	50	3	5256	3.736	0	0.286	0.467	78	0	6	223
		95	3	10008	7.867	0	0	0.015	86	0	13	223
	Oxidant: O_2 + CO, liquid-phase heterogeneously catalyzed reaction, aqueous medium											
12	0.1%–0.5% Rh_1@H-ZSM-5	150	2	243–360	0.244–0.690	2.500–7.000	1.048–0.234	0	6–8	60–70	14	212, 263
13	0.2% Rh_1/dB-ZSM-5	150	0.3	93	0.803	0.352	0.602	0	33	19	3	136
14	0.5% Rh_1–Na/H-ZSM-5	150	2	5	0.143	0.019	0.096	0	55	7	0	212
15	1% Ir_1/@H-ZSM-5	150	2	7	0.125	0.019	0.196	0	37	6	0	138
16	1% Ir_1–$Pd_{0.1}$@H-ZSM-5	150	2	57	0.522	0.108	2.326	0	14	3	20	138
17	1.4% Ir_1–$Pd_{0.1}$–Cu/H-ZSM-5	150	2	29	1.200	0.081	0	0	80	5	15	138
18	0.9% Cu_1@H-SSZ-13			0.6	0.035–0.053	0	0	0	~100	0	0	137
19	0.6% Rh_1/TiO_2		2–5	4	0.077	0	0	0	~100	0	0	212
	Oxidant CO_2, gas-phase heterogeneously-catalyzed reaction											
20	2% Zn_1@H-ZSM-5	300	0.2	3	0	0.200	0.911	0	0	18	0	139
21	2% Zn_1–CeO_2/MMT			0.5–0.6	0	0.600–0.880	0	0	0	100	0	139

Note. The following abbreviations and symbols are used: N–G nitrogen-doped graphene, N–CNT nitrogen-doped carbon nanotubes; dB-ZBM-5 is the deborated zeolite, which was synthesized [136] using boron compounds with subsequent removal of boron from the crystal lattice; therefore, the zeolite was called deborated.

[a] CH_3OOH + $HOCH_2OOH$.

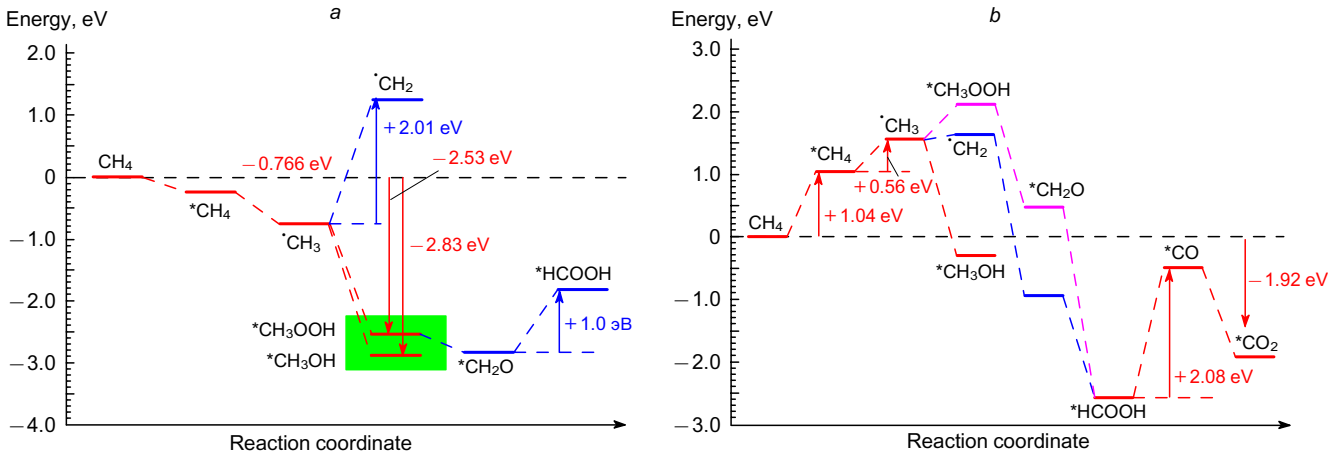

Figure 3. Energy profiles of product formation in the methane oxidation with hydrogen peroxide over the $Rh_1@CeO_2$ single-atom rhodium catalyst (*a*) and Rh_n/CeO_2 nanocluster (*b*). Green colour marks the lowest energy levels; red, blue and lilac colours designate various reaction paths.[202] Published under the Creative Commons Attribution 4.0 International License.

followed by its oxidation to methanol or methyl peroxide[265] (Fig. 3 *a*). Meanwhile, in the presence of Rh_n/CeO_2, the probability of formation of the CH_3 products is relatively low, but a more favourable pathway is the dissociation of the C–H bond in the methyl radical to give the $^{\bullet}CH_2$ intermediate, which is then completely oxidized to CO_2 and CO through HCOOH (Fig. 3 *b*). Therefore, the major products obtained on single-atom sites are CH_3OH and CH_3OOH (where methanol predominates), which are formed at a fairly high rate, whereas over cluster systems (Rh_n/CeO_2), a lot of CO_2 is generated.

A similar trend holds for rhodium-containing compositions [*e.g.*, $Rh_1@ZrO_2$ and Rh_n/ZrO_2 (Ref. 144)] and for copper- and iron-based catalysts [$Cu_1@C_3N_4$ and Cu_n/C_3N_4,[264] $Fe_1@$ZSM-5 and $Fe_n/$H-ZSM-5 (Ref. 268)]. However, in the case of non-noble transition metals, a minor difference was noted, caused by their lower activity compared with the activities of rhodium systems: the reaction product formed on the single-atom sites ($Cu_1@C_3N_4$) was dominated by methyl peroxide, and the process conducted over nanoclusters (Cu_n/C_3N_4) could be suppressed after the formation of HCOOH.

Thus, by varying the nature and the degree of dispersion of the active metal, it is possible to control the selectivity to oxygenates upon the methane oxidation with hydrogen peroxide, which can give either up to 95–100% $CH_3OH + CH_3OOH$ on single-atom metal sites or up to 64–84% HCOOH over nanoclusters.[264, 268]

Recent publications describe the selective formation of not only methanol or formic acid, but also acetic acid (C_2 oxygenate) upon methane oxidation with hydrogen peroxide. This became possible owing to the addition of carbon monoxide to the reaction system [$Rh_1@$H-ZSM-5 (Ref. 220) and Fe/H-ZSM-5 (Ref. 269) catalysts]. The reaction conditions in this case were almost as mild as those used to obtain C_1 oxygenates (T = 50–150 °C).

The benefits of the selective low-temperature oxidative conversion of CH_4 with hydrogen peroxide to C_1 and C_2 oxygenates is beyond doubt, especially when SACs are used. Unfortunately, they are hardly suitable for the industrial implementation due to the high cost of H_2O_2. The search for less expensive oxidants and development of the appropriate single-atom catalytic systems are carried out using both kinetic and computational methods.

According to the results of DFT calculations, selective oxidation of methane to methanol under mild conditions is potentially possible with nitrogen(I) oxide as the oxidant on single-atom sites of a number of metals (Al,[240] Ga,[240] Co,[241] Ti,[243] V [243]) embedded into porous graphene[240, 241] or carbon polynitride ($C_{24}N_{24}$) matrix.[243] With these systems, N_2O is expected to undergo spontaneous decomposition to N_2 and an adsorbed oxygen atom ($^{\bullet}O$), which activates the methane molecule[240, 243]

$$CH_4 + {}^{\bullet}O \longrightarrow [{}^{\bullet}CH_3 + {}^{\bullet}OH] \longrightarrow CH_3OH \qquad (11)$$

As regards the possibility of using air oxygen as a cheap and the most practically convenient oxidant for the reaction with methane, the results of DFT calculations[270] indicate that the activation of the O=O double bond together with the methane activation on a single-atom active site may be difficult. According to estimates,[244, 270] the probability of this pathway increases when the adsorption sites of O_2 and CH_4 molecules are separated (for example, when the $Pd_2/MoCO_2$ diatomic palladium cluster[270] or $Rh_1@$G/Ni(111) complex bimetallic composition[244] is used as the catalyst). The monolayer hexagonal boron nitride doped with a single transition metal atom is considered to be a promising catalyst for the partial methane oxidation:[92] the adsorption of O_2 molecule on this catalyst is likely to give peroxide, the O–O bond of which can be cleaved to give O^- anions, that is, reactive oxygen species for activating CH_4 molecule under mild conditions.

However, only one original method for the activation of oxygen molecule towards the reaction with methane has been practically implemented as yet, that is, a process involving addition of carbon monoxide to the reaction medium.[136–138, 212] This reaction, resulting in the formation of acetic acid and methanol, is called oxidative carbonylation of methane; conduction of this reaction over SACs is studied at several research centres.[136–138, 212, 220, 221, 263, 271–273]

The reaction of CH_4 with O_2 in the presence of CO proceeds as a heterogeneously catalyzed liquid-phase reaction under mild conditions [150 °C, total pressure of 2.7–6.8 MPa, and composition of the reaction mixture,

vol.%: CH_4(2 – 5) + CO(0.5 – 1) + O_2(0.2 – 0.8)] over single-atom catalysts dispersed in an aqueous medium (Rh, Ir, Pd or Cu atoms fixed in a zeolite matrix or on the surface of titanium oxide). This reaction yields oxygenates (methanol, acetic acid, formic acid) at an overall rate of up to 10 000 μmol $g_{cat}^{-1}\,h^{-1}$ with the selectivity to CH_3-containing products ranging from 60 to 100%;[212] the yield of enhanced oxidation products is low (0 – 14% CO_2). In the absence of carbon monoxide, methane oxidation products are not formed on the single-atom catalytic sites.

In the opinion of Moteki *et al.*,[220] carbon monoxide is a co-catalyst of the process (when occurs as a ligand bound to the active metal atom) and also acts as a reducing agent and a reactant. An original hypothetical scheme for the mechanism of methane oxidation with oxygen in the presence of carbon monoxide was proposed (Fig. 4). In relation to the reaction on a rhodium single-atom site, it was stated that the CO ligand located in the coordination sphere of the active metal atom reacts with an oxygen molecule (arriving from the gas phase) to be converted to CO_2, and simultaneously surface metal-oxo compounds are formed. A CH_4 molecule is activated by the oxo species to give Rh – CH_3 and Rh – OH bonds, while the subsequent release of the methoxy form or CO insertion into the Rh – C bond results in the formation of CH_3OH or CH_3COOH, respectively.

According to DFT calculation data,[219] the rate-limiting step of the reaction is the formation of the C – OH bond rather than the activation of CH_4 (the C – OH bond formation is promoted by carbon monoxide, which draws the O_2 molecule into the catalytic cycle). The proposed way of O_2 activation involving CO cannot be called new: it completely agrees with the known facts of effective CO oxidation under mild conditions on the surface of SACs based on noble metals embedded in a zeolite matrix.[274,275]

Moteki *et al.*[220] confirmed experimentally that CO is oxidized to CO_2 with air oxygen over the ZSM-5 zeolite modified with noble metals (rhodium, ruthenium, *etc.*). However, the hypothetical mechanism of methane oxidation catalyzed by the Rh_1@H-ZSM-5 type SAC (see Fig. 4) to give methanol or acetic acid proposed by the authors appears debatable, as this at variance with the low content of CO_2 in the products. The authors themselves agree with this: in their opinion, further spectral studies and analysis of the state of the catalyst surface are required, in order to identify the active sites and intermediates and establish the details of the reaction mechanism.[220]

Meanwhile, according to the proposed scheme (see Fig. 4) and experimental results of other researchers (*e.g.*, Refs 212 and 272), methanol and acetic acid are formed by independent pathways and on different sites, which creates prerequisites for the separate preparation of these products.

Systems containing rhodium immobilized in the H-ZSM-5 type zeolite matrix (with the $SiO_2 : Al_2O_3$ molar ratio of 30 – 300) were studied in most detail.[212,260,263,272,273] It was shown that acetic acid is generated only on single-atom sites, namely, on metal cations possessing high carbonylating activity (*e.g.*, Rh_1^+); only in the presence of BAS, it is formed on the heterogeneous catalytic surface.[212,260,272] A number of chemists[260,272] believe that the zeolite acid sites participate in the oxidation of methane, together with the single-atom rhodium sites: the secondary conversion of methanol (the primary hydrocarbon oxidation product) into acetic acid takes place on zeolite BAS.

According to a viewpoint,[273,276] the zeolite acid sites affect the electronic state of the metal in SACs: the content of BAS in the zeolite influences the electron transfer from the metal (Rh) to the zeolite framework, which was detected by X-ray photoelectron spectroscopy.[273] The fact of interaction between the metal cation and BAS located close to each other in the H-ZSM-5 zeolite matrix was ascertained by Wang *et al.*[207] and Arzumanov *et al.*[233] It was shown that this arrangement of Rh and BAS gives rise to a synergistic effect for the C – H bond activation in the methane molecule [207] and also promotes the formation of acetic acid upon the oxidative carbonylation of methane.[277] In a number of studies,[263,272,273] it was shown using X-ray absorption spectroscopy techniques (EXAFS or XANES) in combination with quantum chemical (DFT) data that single rhodium atoms are fixed in the internal micropores of ZSM-5 type zeolites (in the H-form, H-ZSM-5) *via* the coordination of the metal atom to five oxygen atoms of the zeolite matrix (Rh_1O_5@H-ZSM-5),[244,272] but high activity towards the methane conversion to acetic acid is inherent only in the single-atom systems in which each rhodium atom is bound to five oxygen atoms one of which belongs to the hydroxyl group [Rh_1O_4(OH)]. These sites are mainly formed when the Rh atoms are anchored at channel intersections in the zeolite framework.[273] The single-atom rhodium catalysts enable the preparation of acetic acid by oxidative carbonylation of methane ($CH_4 + CO + O_2$) with a selectivity of 60 – 70% and a specific production rate of up to 420 (g CH_3COOH) $kg_{cat}^{-1}\,h^{-1}$ (Refs 212, 263). These catalysts are superior in performance to all other catalysts known for this reaction,[24,271] including new single-site quasi-homogeneous heterogeneous systems such as Rh_1 – Cu/polyorganic polymer, which are active only upon the addition of a iodine-containing polymer.[51]

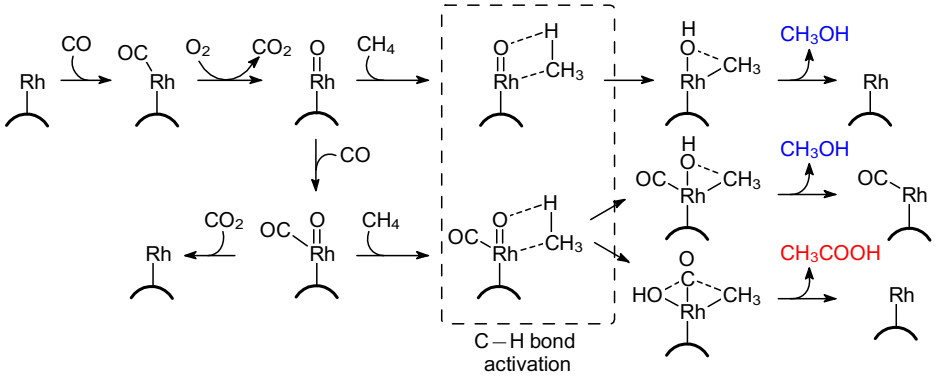

Figure 4. Hypothetical mechanism of methane oxidation with oxygen in the presence of CO on the rhodium single-atom site to form methanol or acetic acid. The blue and red colour marks different reaction products.[220]

Methanol is the main by-product in the oxidative carbonylation of methane to acetic acid. A study of a series of 0.5% Rh_1@H-ZSM-5 catalyst samples with different physicochemical characteristics prepared using impregnation methods with compositionally different polymers in combination with ultrasonic treatment and desilylation [272, 273] demonstrated that methanol, unlike acetic acid, can be formed on cluster metal sites: as the content of rhodium cluster species (Rh – Rh) on the catalyst surface increases, the methanol yield grows, while the yield of acetic acid decreases (Fig. 5 *a*,*b*). The highest selectivity to methanol was observed for a mesoporous catalyst (Fig. 5 *c*), since the location of rhodium in the zeolite mesopores is favourable for the clusterization of metal atoms. As the acidity of the zeolite framework decreases, the methanol selectivity of the 0.5% Rh_1@H-ZSM-5 catalyst also increases (Fig. 5 *d*).

A methanol-selective catalyst can be obtained by using a metal with a low carbonylating activity (Cu, Ir) [137, 138] or by using a narrow-pore zeolite as the support (with the size of the framework cavities corresponding to the kinetic diameter of the CH_3OH molecule), *e.g.*, with CHA [220] or AEI [221] topology (see †). Using both the single-atom Cu_1@H-SSZ-13 and cluster Cu_n/H-SSZ-13 catalytic systems based on copper and the H-SSZ-13 zeolite (CHA topology), methanol is synthesized from CH_4 and $O_2 + CO$ with 100% selectivity, but the SAC activity is 1.5 times higher.[137]

The most efficient single-atom system for methanol synthesis was obtained [138] on the basis of iridium promoted by palladium and copper (to increase the activity and the selectivity, respectively). Methanol is formed over the polymetallic heterogeneous 1.4% Ir_1 – 0.1% Pd_1 – Cu/H-ZSM-5 catalyst upon the methane oxidation with air oxygen (in the presence of CO) at a temperature of 150 °C with a specific production rate of 1.2 (mol CH_3OH) $kg_{cat}^{-1}\,h^{-1}$ at 80% selectivity, which is comparable with these characteristics attained in the synthesis of methanol from CH_4 using expensive H_2O_2 as the oxidant (see Table 3, *cf.* item *17* with items *5* and *11*). In other words, the design of the polymetallic $Ir_1 - Pd_1 - Cu$/H-ZSM-5 single-atom catalyst enables the efficient one-step catalytic synthesis of methanol by oxidation of methane with air oxygen (with carbon monoxide promoting the reaction). This process favourably compares with the recently widely advertised methods of partial oxidation of methane by air oxygen to methanol on zeolites modified with metal-oxo clusters:[158, 278, 279] cluster catalysts are efficient at higher temperatures (not lower than 250 °C), and their performance is moderate; in addition, the chemical looping process design is used most often, that is, two successive stoichiometric reactions are combined.

Recent studies address the possibility of the catalytic oxidation of methane by carbon dioxide to oxygen-

† AEI is the crystalline framework code taken from the Atlas of Zeolite Framework Types, see Note to Table 1 of this review.

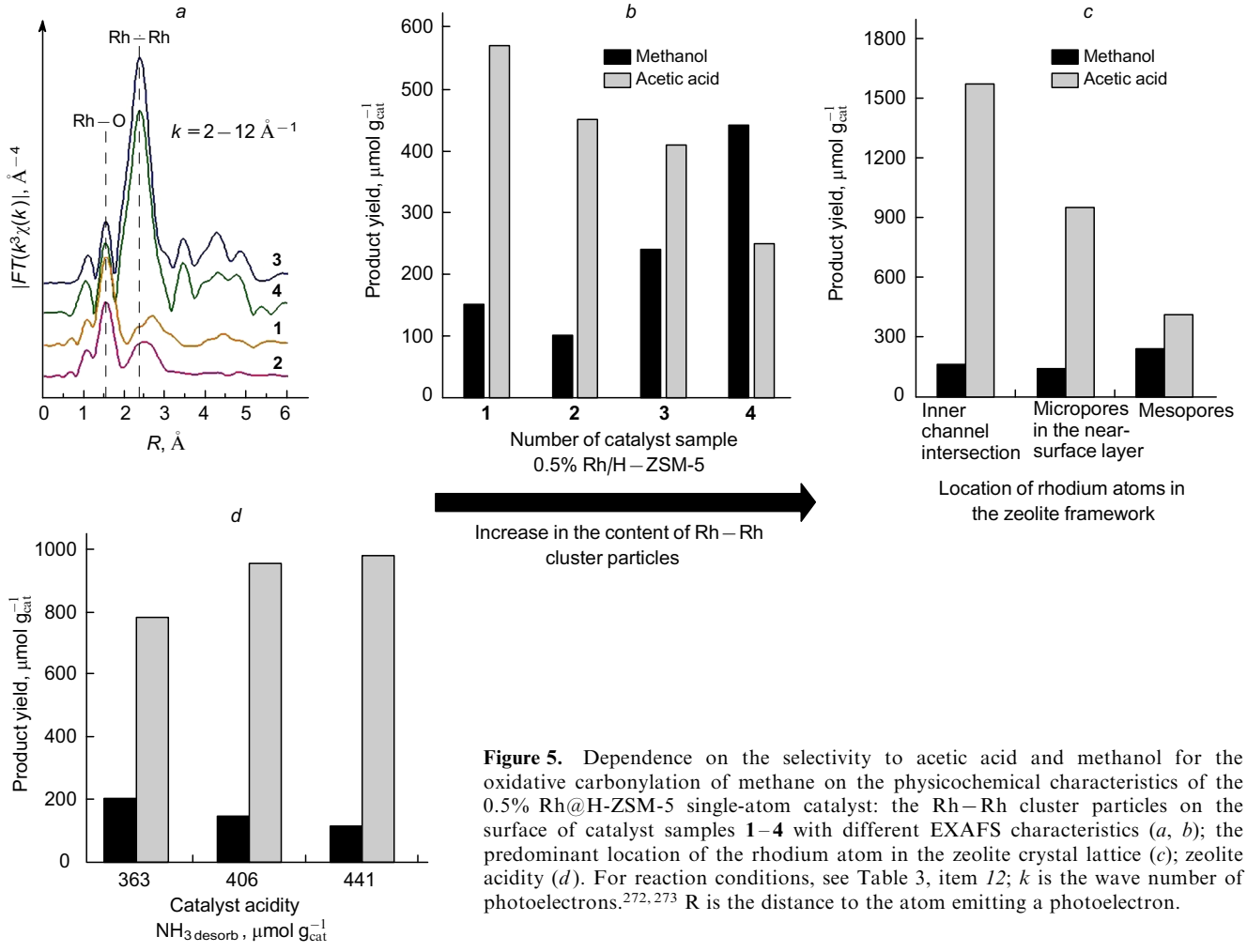

Figure 5. Dependence on the selectivity to acetic acid and methanol for the oxidative carbonylation of methane on the physicochemical characteristics of the 0.5% Rh@H-ZSM-5 single-atom catalyst: the Rh – Rh cluster particles on the surface of catalyst samples **1** – **4** with different EXAFS characteristics (*a*, *b*); the predominant location of the rhodium atom in the zeolite crystal lattice (*c*); zeolite acidity (*d*). For reaction conditions, see Table 3, item *12*; *k* is the wave number of photoelectrons.[272, 273] R is the distance to the atom emitting a photoelectron.

ates,[4,140–143,280,281] including processes involving SACs based on Zn_1,[175,188] Zr_1,[281] Pt_1[188] and Ag_1.[141] The supports used for such systems are zeolites (most often, H-ZSM-5)[139,232] or metal oxides (CeO_2,[139,141] In_2O_3,[142] ZnO[143]). The reaction of CH_4 with CO_2 is carried out at moderate temperatures ($\geqslant$ 300 °C), *i.e.*, under more drastic conditions than methane oxidation reactions with other oxidants (H_2O_2, O_2 + CO), which is due to high strength of the C=O bonds of the CO_2 molecule; the activation energy of the carbon dioxide molecule (532 kJ mol^{-1}) is higher than that of the methane molecule (435 kJ mol^{-1}). The target product of the reaction is acetic acid. No methanol is formed, but formic acid may appear as a by-product (see Table 3, items *20*, *21*).

The most active single-atom catalyst for the reaction of CH_4 with CO_2, as well as with other oxidants, is formed using ZSM-5 type zeolite (in this case, Zn_1@H-ZSM-5).[139,232] However, the selectivity of this catalyst to acetic acid is very low (18%),[139] while formic acid is the major reaction product (82% selectivity). It is believed [4,232] that this is caused by the difficulty of C–C bond formation on a monometallic site.

In a series of studies [139–143,218] performed using mainly quantum chemical calculations, it was demonstrated that an efficient catalyst for the methane oxidation with carbon dioxide to acetic acid can be formed only provided that the activation sites of reactants (CH_4 and CO_2) are separated. On the basis of DFT calculation results,[141] it was recommended to use binary catalytic systems consisting of a single-atom metal site (to activate the CH_4 molecule) and a metal oxide (to activate the CO_2 molecule as a frustrated Lewis pair). The frustrated pair (acid and base) Lewis sites can be formed spontaneously upon the deposition of single metal atoms onto the surface of some oxides [CeO_2,[141] In_2O_3 (Ref. 142)] owing to the formation of oxygen vacancies. High efficiency is predicted for the following binary systems: Ag_1/CeO_2,[141] Zr_1/In_2O_3,[142] Fe_1/ZnO.[143] The efficiency of the Zn_1/CeO_2 system was confirmed by kinetic experiment.[139,218] Using the catalyst obtained upon the deposition of this binary system on montmorillonite, acetic acid was prepared, with the specific production rate being 0.6–0.9 mol kg_{cat}^{-1} h^{-1} at 100% selectivity.[139] The reaction of CH_4 with CO_2 was conducted as a gas-phase heterogeneously catalyzed process at an equimolar ratio of the reactants, a temperature of 300 °C and a total pressure of 0.2 MPa.

Thus, using SACs efficient in the direct oxidative conversion of methane and readily available oxidants (CO_2, H_2O_2, O_2 + CO) can provide a low-temperature (or, at least, medium-temperature) selective synthesis of CH_3-containing oxygenates (methanol, acetic acid). The highest activity was noted for the catalytic systems with the active metal immobilized into a zeolite framework. The bimetallic or polymetallic systems are more selective in the methane conversion to methanol (with H_2O_2 and O_2 + CO as oxidants) and in the methane carboxylation to acetic acid. In the oxidative carbonylation of methane to acetic acid on single-atom rhodium sites, only monometallic catalysts have been studied so far.

In the oxidative processes described above, the C_2 product (acetic acid) is formed *via* the C–C bond formation involving carbon oxides (CO_2 or CO). Meanwhile, there is another way for the formation of the carbon skeleton upon coupling of the CH_4 molecules, which results in the formation of C_{2+} hydrocarbons.

5. Direct conversion of methane into hydrocarbons

Direct conversion of methane under non-oxidative conditions results in the formation of ethane (ethylene) and aromatic hydrocarbons (benzene, toluene, naphthalene).[5,6,45,46,147,282–285] The chemical conversion of CH_4 is implemented *via* successive dehydrogenation of the methane molecule in combination with the condensation processes of carbon-containing products. This transformation includes the activation of the C–H bonds of the methane molecule on the catalyst surface to give the $^{\bullet}CH_3$, $^{\bullet}CH_2$ and $^{\bullet}CH$ species, which then undergo recombination to give C–C bonds either in the gas phase[23,284,285] or on the catalyst surface.[5,282] By varying the reaction conditions and composition of the heterogeneous catalyst, it is possible to terminate the carbon chain growth at a definite stage and to direct the process along the desired pathway, thus providing the selective formation of the target hydrocarbon product: ethane (ethylene) or benzene (toluene). The difficulty of the successful solution of this problem is associated with the thermodynamic factors, which dictate that conversion of methane to polyaromatic compounds (naphthalene and coke structures) is more favourable than the conversion to C_2, C_6 or C_7 hydrocarbons over the whole range of applicable temperatures (at least up to 950 °C).[5,285]

The good prospects for the application of SACs in these processes is obvious: stabilization of the methyl groups upon the activation of methane characteristic of these heterogeneous catalytic systems may retard the propagation of the carbon chain and, hence, the undesirable extensive condensation processes would be suppressed.

The data on SACs used in non-oxidative conversion of CH_4 by methane dehydroaromatization (DHAM) to give benzene,[286–291] benzene methylation with methane (MBM) to give toluene[132–135] and non-oxidative coupling of methane (NOCM) to give C_2 hydrocarbons (ethane or ethylene) are summarized in Table 4. In most of the known examples, the single-atom metal sites are stabilized by the zeolite framework with ten-membered (10MR) channels (ZSM-5,[132–135,287–292] ZSM-11[135] and MCM-22[294,295] zeolites), which ensure the shape selectivity of the catalyst to hydrocarbons with up to 10–12 carbon atoms.

The catalytic systems for methane dehydroaromatization are obtained, as a rule, using molybdenum.[295–297] Until recently, only heterogeneous catalysts containing metal clusters of low nuclearity, mainly Mo_n/H-ZSM-5 (n = 4–6), were used in this reaction.[282–284,288] It is believed [282,286] that C–H bond activation in the methane molecule and formation of the C–C bonds can occur simultaneously on the cluster species, while aromatization of the resulting fragments occurs in micropores in the zeolite matrix. Methane conversion to a number of aromatic compounds (a mixture of benzene, toluene, naphthalene and coke) takes place over the catalysts containing molybdenum nanoclusters at temperatures of 700–750 °C; the product also contains ethane and ethylene impurities. The benzene selectivity does not exceed 50%; polyaromatic compounds and coke are intensely formed and, hence, the catalyst is rapidly deactivated.

The behaviour of molybdenum catalysts with single metal atoms in the DHAM reaction has been studied.[286–291] Two forms of heterogeneous catalysts have been tested, those with a single-atom molybdenum site[286] and with a single-atom sites of other transition metals introduced into

Table 4. Direct methane conversion to hydrocarbons over single-atom catalysts.

No	Catalyst [a]	Reaction conditions			Specific reaction rate, mmol g_{cat}^{-1} h^{-1}		CH_4 conversion (%)	Toluene yield (%)	Selectivity (%)					Ref.
		T, °C	*p*, MPa	*t*, h	CH_4 consumption	Ethane + ethylene formation			C_2-hydrocarbons [b]	benzene	toluene	naphthalene	coke	
					Dehydroaromatization of methane: n CH_4 → H_2 + C_6H_6 + ... + $C_{10}H_8$									
1	2–6% Mo_n/H-ZSM-5	700–750	0.1	1–16	up to 1.9	0.06	8–12	–	2–3.5	46–50	1–3	10–35	~30	282–284
2	2% Mo_1@H-ZSM-5	700	0.1	1–6	–	–	~7	–	–	~60	–	–	<15	286
3	0.5% Re_1–4% Mo_n/H-ZSM-5	750	0.1	1–13	–	0.10	14	–	3	46–50	–	32	–	287, 288
4	0.2% Fe_1–4% Mo_n/H-ZSM-5	700	0.1	1–12	–	–	10	–	<3	75–83	–	–	<7	289, 290
5	0.5% Ru_1–2% Mo_n/H-ZSM-5	700–750	0.1	1–16	–	–	8.5	–	2	61	6.5	25	6	291
6	0.5% Pd_1–2% Mo_n/H-ZSM-5	700–750	0.1	1–16	–	–	7	–	1	66	9	15.5	9	291
7	0.5% Pt_1–2% Mo_n/H-ZSM-5	700	0.1	0.5–6	–	–	7	–	1.5	71	5	14	9.5	291
					Methylation of benzene with methane: 7 CH_4 → 10 H_2 + $C_6H_5CH_3$									
8	Mo_1@H-ZSM-5	570	–	–	0.2	–	–	–	–	–	60	–	–	132
9	Pt_1@H-ZSM-5	570	–	–	5.9	–	–	–	–	–	60	–	–	132
10	Rh_1@H-ZSM-5	570	–	–	4.7	–	–	–	–	–	40	–	–	132
11	Pd_1@H-ZSM-5	570	–	–	4.3	–	–	–	–	–	30	–	–	132
12	Co_1@H-ZSM-5	570	–	–	1.9	–	–	1.7	–	–	50	–	–	133
13	Co_1@H-ZSM-5	500	–	4	–	–	–	0.3	–	–	–	–	–	134, 135
14	Co_1–Mg/H-ZSM-5	500	–	4	–	–	–	1.1	–	–	–	–	–	134
15	Co_1–Ce/H-ZSM-5	500	–	4	–	–	–	1.4	–	–	–	–	–	134
					Non-oxidative coupling of methane to C_2-hydrocarbons: n CH_4 → H_2 + C_2H_6 + C_2H_4									
16	H-Ta_1($SiO)_2$	475	5.0	1	–	–	0.5	–	>98	–	–	–	–	235
17	1%Pt–0.8%Bi/H-ZSM-5	650	0.01	1	–	–	4–5.5	–	~94	~3	–	–	~3	292
18	GaN/SBA-15 (see [c])	700	0.1	1–8	1.5–2.0	–	0.5–2	–	97–98	0.1–0.4	–	–	–	146
19	0.5% Pt_1@CeO_2	975	0.1	40	–	–	14	–	74	13	–	2	~1	146, 285
20	0.5% Fe_1@SiO_2	1020–1090	0.1	60	69–104	–	32–48	–	48–54	20–28	–	24–25	–	293

Note. *p* is pressure, *t* is the reaction time. For catalysts *17*, *19* and *20*, TOF values were found to be 162, 18 and 773–1165 h^{-1}, respectively. [a] The metal content is given in (mass %); [b] ethane + ethylene + acetylene; [c] SBA-15 (Santa Barbara Amorphous-15) is a mesoporous silica with large internal surface area.

the molybdenum nanocluster precursor (M_1-Mo_n/H-ZSM-5, where M is a transition metal).[287–291] In all cases, switching from nanocluster systems to single-atom catalysts was accompanied by a considerable (~2–6-fold) decrease in the coke formation rate and increase in the catalyst stability, selectivity and yield of benzene (the target product). However, the activity of the monometallic single-atom Mo_1@H-ZSM-5 catalyst was noted to be lower than that of nanocluster analogues (*cf.* items *1* and *2* in Table 4).

The catalytic systems efficient in all respects were obtained as bimetallic species by doping the molybdenum cluster by single-atom sites of another transition metal (Re, Fe, Pt, Pd, Ru).[287–291] The highest activity was found for bimetallic systems containing rhenium as the dopant — Re_1-Mo_4/H-ZSM-5.[287,288] This was explained [288] by acceleration of the C–C bond formation by the action of the Re–Mo metal pair. This is evidenced by the fact that the rate of ethane formation from CH_3 fragments increases twofold when the initial molybdenum catalyst is modified with rhenium. The most selective and stable catalyst was obtained by doping the molybdenum system with single-atom iron.[289,290] In the presence of the Fe_1-Mo_n/H-ZSM-5 catalysts, benzene is formed at a high constant rate and with a selectivity of up to 83%; the methane conversion reaches equilibrium values (10–12%), while the catalyst operation time is at least 10 h. Unlike the iron-containing system, bimetallic molybdenum-containing catalysts modified with noble metal atoms (Pt, Pd, Ru) [291] are less stable, but in the presence of these catalysts, the formation of aromatic compounds from methane proceeds with high total selectivity (~90%); apart from benzene (61–71%), the reaction products contain a considerable concentration (5–9%) of toluene, an important petrochemical hydrocarbon.

Katada and co-workers [132–135] demonstrated that toluene can be synthesized by the MBM reaction at temperatures of 500–570 C using SACs based on some transition metals (Pt, Pd, Rh, Co) embedded into the H-ZSM-5 zeolite matrix. In these systems, the single-atom metal sites activate CH_4 to give methyl species, while the zeolite acid sites participate in benzene activation. As can be seen from the data presented in Table 4 (items *8–15*), the Mo_1@H-ZSM-5 single-atom catalyst has virtually no activity in this reaction (this apparently accounts for the low content of toluene in the DHAM reaction products). Meanwhile, when SACs based on noble metals (Pt_1@H-ZSM-5, Pd_1@H-ZSM-5, Rh_1@H-ZSM-5) are used, toluene is formed at a high initial rate, which is 2–3 times higher than the rate of the DHAM reaction. However, due to the agglomeration of metal particles, these catalytic systems are rapidly deactivated during the MBM reaction.

The stability of cobalt-based SACs is markedly higher. For example, in the presence of Co_1@H-ZSM-5 at 500 °C, toluene is produced from CH_4 and C_6H_6 at a constant rate (156 $\mu mol\, g_{cat}^{-1}\, h^{-1}$) for at least 4 h, while the reaction rate in the presence of Pt_1@H-ZSM-5 decreases over the same period from 414 to 30 $\mu mol\, g_{cat}^{-1}\, h^{-1}$ (Refs 132, 133). The introduction of a second metal (M = Mg, Ca, Zn, Pb, Ni, Ce) [134] into Co_1@H-ZSM-5 additionally stabilizes the single-atom active sites — Co^{2+} cations;[133,135] as a result, on going to bimetallic Co_1-M/H-ZSM-5 systems, the yield of toluene can be increased 3–5-fold. An important role in the catalytic process is played by the shape selectivity of the zeolite support, which should match the kinetic diameter of benzene and toluene molecules. Considering this fact, effective catalysts are obtained on the basis of zeolites with MFI morphology (ZSM-5, ZSM-11),[135] while immobilization of cobalt atoms into the MOR, BEA or FAU (fojasite crystal structure) crystalline framework results in absolutely inert systems.[133]

In the methane conversion under non-oxidative conditions, it is most difficult to obtain C_2 hydrocarbons (ethane, ethylene) by arresting the condensation processes in the initial stage (NOMC reaction).[298,299] However, exactly SACs can cope with this challenge.

A variety of SACs have been used for the NOMC reaction (see Table 4, items *16–20*). It was reported that ethane is formed with >90% selectivity in the presence of H-$Ti_1(SiO)_2$ (Ref. 235) and Pt_1-Bi/H-ZSM-5 systems (bimetallic catalyst) [292] and that ethylene is formed selectively (97%) in the presence of the GaN/SBA-15 gallium nitride catalyst.[145] Using these SACs, the reactions are carried out at moderate temperatures (475–700 °C); the catalyst activity is relatively high: the turnover frequency of the metal site is $>160\ h^{-1}$, and the reaction rate is not lower than the rate of methane dehydroaromatization or benzene methylation (*cf.* items *1*, *12* and *18* in Table 4). However, the attained yield of the C_2 products is moderate (0.5–5%), apparently, due to the severe thermodynamic limitations in this temperature range.[146]

The equilibrium values of methane conversion to C_2 hydrocarbons acceptable for practical use (at ~20% level) can be attained only at temperatures of >950 °C;[285] therefore, high-temperature single-atom heterogeneous catalysts, Pt_1@CeO_2 (Refs 146, 285) and Fe_1@SiO_2,[293,300–303] were developed for conducting the NOMC reaction under drastic conditions. The methane conversion over the Pt_1@CeO_2 platinum sites at 975 °C is ~14%; the hydrocarbon products are dominated by C_2 compounds (74%), but with a high percentage of acetylene (35% C_2H_2) and lower percentages of ethane and ethylene (6% C_2H_6, 33% C_2H_4).[146,285] The single-atom Fe_1@SiO_2 iron sites are more efficient: the ethylene selectivity reaches 45–48% (the other products are benzene and naphthalene); at a temperature of 1090 °C, the conversion of methane is 48%.[293] According to the results of DFT calculations,[300] a more efficient catalyst can be produced by incorporating a tungsten atom, instead of iron, into the silica matrix. However, the W_1@SiO_2 system has not yet been tested experimentally.

Only the Fe_1@SiO_2 single-atom catalyst is of interest considering the potential commercialization: over this catalyst, ethylene is formed in 25% yield, the reaction is stable and the catalyst operation time exceeds 60 h. Currently, studies are carried out to test various designs of NOMC process with this catalytic system (in particular, using a membrane reactor with a hydrogen-permeable membrane [301] and an iron quartz reactor).[302,303] Simultaneously, details of the reaction mechanism are being studied; the reaction is assumed to follow a radical mechanism.[303–306] The isolated nature of the single active sites prevents the catalytic C–C coupling of the $^{\bullet}CH_3$ and $^{\bullet}CH_2$ species formed in the initial stage. At a high reaction temperature, these species rapidly diffuse from the catalytic surface and undergo recombination in the gas phase; this provides a high selectivity of the reaction to the C_2 hydrocarbons.[293] As it was shown,[285,293] this effect cannot be attained using nanocluster-based catalysts: the use of heterogeneous Fe_n/SiO_2 (T = 1020 °C) and Pt_n/CeO_2 (T = 975 °C) catalysts leads to the predominant

(80 – 100% selectivity) formation of coke, resulting from enhanced condensation; the catalyst loses activity in the first minutes of the process, and the yields of C_2 hydrocarbons do not exceed 0.3%.[285, 293]

Thus, the use of single-atom catalysts in the NOMC reaction, like in the syntheses of aromatic hydrocarbons (DHAM, MBM), can be regarded as a key to the selective stable preparation of the target hydrocarbons from methane under non-oxidative conditions. Which of the products, ethane (ethylene) or benzene (toluene), would be formed in a larger amount, depends on the type of single-atom heterogeneous catalyst used and on the reaction temperature. For the synthesis of C_2 hydrocarbons, it is most appropriate to combine the use of a single-atom monometallic site on an oxide support and a high (> 950 °C) temperature of the reaction for fast removal of the primary intermediates formed on the single-atom metallic site from the catalyst surface; this makes it possible to terminate the coupling in an initial stage. The aromatic hydrocarbons are efficiently obtained at lower temperatures (570 – 750 °C) on bimetallic catalytic systems of a complex size composition. These systems contain single atoms of one metal, which activate CH_4, and nanoclusters of another metal immobilized in the zeolite framework (usually H-ZSM-5 type), which provide the formation of the C_{2+} carbon skeleton needed for dehydroaromatization of the obtained hydrocarbon chain. The separate (selective) synthesis of these two groups of hydrocarbon products is possible, despite the common mechanism of activation of the primary C – H bond of methane, owing to the difference between the mechanisms of C – C bond formation: a radical gas-phase process gives ethane (ethylene), while the growth of the carbon skeleton on the heterogeneous catalytic surface involving nanocluster metal species leads to the production of benzene (toluene), provided that the subsequent dehydroaromatization of the resulting hydrocarbon chain takes place.

A common drawback of all processes of methane conversion to hydrocarbons under non-oxidative conditions is their exceptionally unfavourable thermodynamic characteristics at low and moderate temperatures. Unfortunately, the use of single-atom heterogeneous catalysts does not turn these processes into low-temperature ones. Meanwhile, a decrease in the reaction temperature may be attained by adding an oxidant (air oxygen) to the reactant mixture. For example, the oxidative coupling of methane is carried out at temperatures of 410 – 780 °C over nanostructured heterogeneous catalysts based on lanthanum oxide; this results in the formation of C_2 hydrocarbons with 45 – 73% selectivity.[23, 58, 307] The conceptual possibility was demonstrated for selective preparation of ethane from a $CH_4 + O_2$ mixture (300 : 1 v/v) *via* a heterogeneously catalyzed gas-phase process over the $Rh_1@ZrO_2$ single-atom rhodium catalyst at a moderate temperature (260 °C) and an atmospheric pressure.[144] In the case of nanoclusters of the same composition (Rh_n/ZrO_2) under similar conditions, only CO_2 is formed. Hence, the use of SACs suppresses deep oxidation, *i.e.*, this solves the key problem of the oxidative methane conversion, that is, high thermal lability of the primary products of CH_4 oxidation. The above-cited publication [144] is still the only one example of low-temperature methane coupling to C_2 hydrocarbons over SACs; however, the results attained by the authors attest to good prospects of these catalytic systems in the oxidative coupling of methane.

6. Conclusion

The use of single-atom catalysts for the activation of stable CH_4 molecule opens up new prospects in methane chemistry, namely:

— there appears the possibility of one-step heterogeneously catalyzed selective conversion of CH_4 to oxygenates and hydrocarbons containing a methyl group (methanol, acetic acid, ethane);

— the inclusion of single-atom metal sites into heterogeneous catalytic systems may decrease the reaction temperature (by at least 200 °C) and thus suppress the undesirable side reactions that give polyaromatic compounds and coke and sharply increase the catalyst operation time in the methane reforming and dehydroaromatization processes;

— single-atom catalysts demonstrated a high potential virtually in all reactions of direct methane conversion; their appearance opened up the first real possibility for the design of low-temperature selective processes for single-stage methane conversion into a wide range of value-added chemicals (synthesis gas, methanol, acetic acid, ethane, ethylene, benzene, toluene).

On the basis of analysis of the published experimental data and the mechanistic details of the conversion of methane and co-reactants (O_2, H_2O, CO_2, benzene) to the target products, it is possible to give some recommendations concerning the use of one or another type of single-atom catalyst in the particular methane conversion process. For example, systems of a complex size composition that include both SACs and nanoclusters (of the same or another transition metal) are needed in two cases:

— if apart from CH_4 activation, the formation of C_{2+} carbon skeleton (methane dehydroaromatization) is required;

— if the co-reactant (H_2O, O_2) of methane is activated only on cluster metal sites, but is not activated on SACs (methane steam reforming and partial oxidation to synthesis gas).

Bimetallic systems with single-atom sites of two different metals are efficient for the reactions that involve CH_4 and CO_2, which are activated according to different principles (dry reforming, methane carboxylation into acetic acid). Meanwhile, in those cases where the catalytic cycle can be accomplished with only one metal site [methane oxidation and oxidative carbonylation, non-oxidative coupling to ethane (ethylene), or methylation of benzene with methane], a second metal can also be introduced into the catalytic composition in order to increase the stability of the single-atom sites of the active metal or to affect the catalyst selectivity.

It is also noteworthy that almost in cases, the most active and selective single-atom catalytic systems (both mono- and bimetallic) are obtained by immobilization of active metal sites in a zeolite matrix (mainly, H-ZSM-5 type): metal immobilization in the micropores of a structured support provides a uniform distribution of metal active sites over the catalytic surface; most often, they exist as cations acting as sites for the low-temperature activation of CH_4.

Unfortunately, there are still few publications on the application of these promising catalytic systems in each particular reaction of CH_4 (this is especially true for the methane reforming and methylation and for the reaction of CH_4 with CO_2 to give acetic acid). Hence, it is necessary to intensify the studies in this field in the near future.

The present review, devoted to a new promising area of chemistry, transformations of the stable methane molecule over single-atom catalysts, is meant for a wide circle of researchers engaged in the development of new efficient catalysts for reactions involving methane. We hope that this information would also be of interest for higher school teachers, post-graduates and students.

This work was performed with the financial support of the Russian Science Foundation (Grant No. 21-73-20042).

7. List of abbreviations and symbols

BAS — Brønsted acid sites,
DFT — density functional theory,
DHAM — dehydroaromatization of methane,
EXAFS — extended X-ray absorption fine structure,
G — graphene,
HAP — hydroxyapatite,
HRTEM —high-resolution transmission electron microscopy,
MBM — methylation of benzene with methane,
NOMC — non-oxidative methane coupling,
OCM — oxidative coupling of methane,
R — the distance to the atom emitting a photoelectron
SACs — single atom catalysts,
SBA-15- — mesoporous crystalline silica (Santa Barbara Amorphous-15),
TOF — turnover frequency,
XAS — X-ray absorption spectroscopy,
XANES — X-ray absorption near edge structure,
ZSM-5 — Zeolite Socony Mobil-5,
ZSM-11 — Zeolile Socony Mobil-11 (MEL).

8. References

1. P.Schwach, X.Pan, X.Bao. *Chem. Rev.*, **117**, 8497 (2017); https://doi.org/10.1021/acs.chemrev.6b00715
2. A.I.Olivos-Suarez, A.Szecsenyi, E.J.M.Hensen, J.Ruiz-Martinez, E.A.Pidko, J.Gascon. *ACS Catal.*, **6**, 2965 (2016); https://doi.org/10.1021/acscatal.6b00428
3. R.Sharma, H.Poelman, G.B.Marin, V.V.Galvita. *Catalysts*, **10**, 194 (2020); https://doi.org/10.3390/catal10020194
4. Ch.Tu, X.Nie, J.G. Chen. *ACS Catal.*, **11**, 3384 (2021); https://doi.org/10.1021/acscatal.0c05492
5. T.Y.Zhang. *Chem. Sci.*, **12**, 12529 (2021); https://doi.org/10.1039/D1SC02105B
6. S.V.Konnov. *Petrol. Chem.*, **62**, 280 (2022); https://doi.org/10.1134/S0965544122010017
7. H.Song, J.Jarvis, Sh.Meng, H.Xu, Zh.Li, W.Li. In *Methane Activation and Utilization in the Petrochemical and Biofuel Industries: Introducing Methane Activation. Ch. 2*. (Cham: Springer, 2022). P. 23; https://doi.org/10.1007/978-3-030-88424-6_2
8. N.Salahudeen, A.A.Rasheed, A.Babalola, A.U.Moses. *J. Natur. Gas Sci. Eng.*, **108**, 104845 (2022); https://doi.org/10.1016/j.jngse.2022.104845
9. E.E.Claveau, S.Sader, B.A.Jackson, S.N.Khan, E.Miliordos. *Phys. Chem. Chem. Phys.*, **25**, 5313 (2023); https://doi.org/10.1039/D2CP05480A
10. L.S.Andrade, H.H.L.B.Lima, C.T.P.Silva, W.L.N.Amorim, J.G.R.Poco, A.López-Castillo, M.V.Kirillova, W.A.Carnalho, A.M.Kirillov, D.Mandelli. *Coord. Chem. Rev.*, **481**, 215042 (2023); https://doi.org/10.1016/j.ccr.2023.215042
11. C.Karakaya, R.J.Kee. *Prog. Energy Combust. Sci.*, **55**, 60 (2016); https://doi.org/10.1016/j.pecs.2016.04.003
12. W.Taifan, J.Baltrusaitis. *Appl. Catal.*, B, **198**, 525 (2016); https://doi.org/10.1016/j.apcatb.2016.05.081
13. M.V.Popov, A.G.Bannov, A.E.Brester, P.B.Kurmashov. *Russ. J. Appl. Chem.*, **93**, 954 (2020); https://doi.org/10.1134/S1070427220070022
14. M.A.Gubanov, M.I.Ivantsov, M.V.Kulikova, M.I.Knyazeva, A.B.Kulikov, A.L.Maksimov, V.A.Kryuchkov, Nikitchenko, A.A.Pimenov. *Petrol. Chem.*, **60**, 1043 (2020); https://doi.org/10.1134/S096554412009011X
15. S.M.Aldoshin, V.S.Arutyunov, V.I.Savchenko, I.V.Sedov, A.V.Nikitin, I.G.Fokin. *Russ. J. Phys. Chem. B*, **15**, 498 (2021); https://doi.org/10.1134/S1990793121030039
16. V.S.Arutyunov, A.V.Nikitin, V.I.Savchenko, I.V.Sedov. *Catal. Industry*, **14**, 1 (2022); https://doi.org/10.1134/S2070050422010020
17. I.V.Bilera, N.N.Buravtsev, I.V.Rossikhin. *Russ. J. Appl. Chem.*, **93**, 456 (2020); https://doi.org/10.1134/S1070427220030180
18. E.Busillo, V.S.Arutyunov, V.I.Savchenko. *Petrol. Chem.*, **61**, 1228 (2021); https://doi.org/10.1134/S0965544121110037
19. V.I.Savchenko, Ya.S.Zimin, A.V.Nikitin, I.V.Sedov, V.S.Arutyunov. *Russ. J. Appl. Chem.* **95**, 11991206 (2022); https://doi.org/10.1134/S107042722208016X
20. A.Nikitin, A.Ozersky, V.Savchenko, I.Sedov, V.Arutyunov, V.Shmelev. *Chem. Eng. J.*, **377**, 120883 (2019); https://doi.org/10.1016/j.cej.2019.01.162
21. V.I.Savchenko, A.V.Ozerskii, I.G.Fokin, A.V.Nikitin, V.S.Arutyunov, I.V.Sedov. *Russ. J. Appl. Chem.*, **94**, 509 (2021); https://doi.org/10.1134/S107042722104011X
22. I.V.Kudinov, A.A.Pimenov, G.V.Mikheeva. *Petrol. Chem.*, **60**, 1239 (2020); https://doi.org/10.1134/S0965544120110122
23. N.V.Kolesnichenko, N.N.Ezhova, Yu.M.Snatenkova. *Russ. Chem. Rev.*, **89**, 191 (2020); https://doi.org/10.1070/RCR4900
24. N.N.Ezhova, N.V.Kolesnichenko, A.L.Maximov. *Petrol. Chem.*, **62**, 40 (2022); https://doi.org/10.1134/S0965544122010078
25. K.B.Golubev, O.V.Yashina, N.N.Ezhova, N.V.Kolesnichenko. *Mendeleev Commun.*, **31**, 712 (2021); https://doi.org/10.1016/j.mencom. 2021.09.040
26. A.A.Stepanov, L.L.Korobitsyna, A.V.Vosmerikov, R.Z.Kuvatova, O.S.Travkina, B.I.Kutepov. *Petrol. Chem.*, **61**, 370 (2021); https://doi.org/10.1134/S0965544121020092
27. Z.V.Budaev, E.P.Meshcheryakov, I.A.Kurzina, A.V.Vosmerikov, L.L.Korobitsyna. *Petrol. Chem.*, **61**, 1234 (2021); https://doi.org/10.1134/S0965544121110025
28. A.R.Osipov, V.A.Borisov, V.L.Temerev, D.A.Shlyapin. *Petrol. Chem.*, **61**, 1243 (2021); https://doi.org/10.1134/S0965544121110104
29. V.V.Nedolivko, G.O.Zasypalov, A.V.Vutolkina, P.A.Gushchin, V.A.Vinokurov, S.V.Egazaryants, A.P.Glotov, L.A.Kulikov, E.A.Karakhanov, A.L.Maksimov. *Russ. J. Appl. Chem.*, **93**, 765 (2020); https://doi.org/10.1134/S1070427220060014
30. T.A.Kryuchkova, V.V.Kost, T.F.Sheshko, I.V.Chislova, L.V.Yafarova, I.A.Zvereva. *Petrol. Chem.*, **60**, 609, (2020); https://doi.org/10.1134/S0965544120050059
31. E.G.Chepaikin,G.N.Menchikova, S.I.Pomogailo. *Russ. Chem. Bull.*, **68**, 1465 (2019); https://doi.org/10.1007/s11172-019-2581-5
32. X.Meng, X.Cui, N.P.Rajan, L.Yu, D.Deng, X.Bao. *Chem*, **5**, 2296 (2019); https://doi.org/10.1016/j.chempr.2019.05.008
33. Z.Zhu, W.Guo, Y.Zhang, Ch.Pan, J.Xu, Y.Zhu, Y.Lou. *Carbon Energy*, **3**, 519 (2021); https://doi.org/10.1002/cey2.127
34. X.Cui, R.Huang, D.Deng. *Energy Chem.*, **3**, 100050 (2021); https://doi.org/10.1016/j.egyai.2021.100050
35. L.L.Sun, Y.Wang, N.J.Guan, L.D.Li. *Energy Technol.*, **8**, 1900826 (2020); https://doi.org/10.1002/ente.201900826
36. V.I.Lomonosov, M.Yu.Sinev. *Kinet. Catal.*, **62**, 103 (2021); https://doi.org/10.1134/S0023158420060063
37. V.S.Arutyunov. *Direct Methane to Methanol: Foundations and Prospects of the Process*. (Amsterdam: Elsevier, 2014). P. 309; https://doi.org/10.1016/C2012-0-06330-2

38. B.V.Arutyunov. *Rev. Chem. Eng.*, **37**, 99 (2021); https://doi.org/10.1515/revce-2018-0057
39. A.S.Loktev, A.A.Sadovnikov, A.K.Osipov, A.G.Dedov, I.E.Mukhin, M.A.Bykov. *Petrol. Chem.*, **62**, 526 (2022); https://doi.org/10.1134/S0965544122020207
40. T.I.Batova, T.K.Obukhova, A.N.Stashenko, E.E.Kolesnikova, N.V.Kolesnichenko. *Petrol. Chem.*, 62, 425 (2022); https://doi.org/10.1134/S0965544122020165
41. D.Zeng, Ch.Wang, T.Liu, W.Ou, R.Xiao. *Fuel Proc. Technol.*, **234**, 107320 (2022); https://doi.org/10.1016/j.fuproc.2022.107320
42. N.Sun, J.Zhang, L.Ling, R.Zhang, D.Li, B.Wang. *J. Phys. Chem. C*, **126**, 4306 (2022); https://doi.org/10.1021/acs.jpcc.1c04670
43. Zh.Ch.Xu, E.D.Park. *Catalysts*, **12**, 314 (2022); https://doi.org/10.3390/catal12030314
44. Th.Imyen, E.Znoutine, D.Suttipat, P.Ladrat, P.Kidkhunthod, S.Bureekaew, Ch.Wattanakit. *ACS Appl. Mater. Interfaces*, **12**, 23812 (2020); https://doi.org/10.1021/acsami.0c02273
45. Á.López-Martín, A.Caballero, G.Colón. *Appl. Catal. B*, **312**, 121382 (2022); https://doi.org/10.1016/j.apcatb.2022.121382
46. H.Song, J.Jarvis, S.Meng, H.Xu, Z.Li, W.Li. In *Methane Activation and Utilization in the Petrochemical and Biofuel Industries: Direct Systems: Methane Dehydroaromatization (MDA) and the Oxidative Coupling of Methane (OCM). Ch. 3*. (Cham: Springer, 2022). P. 43; https://doi.org/10.1007/978-3-030-88424-6_3
47. Y.Tang, Y.Li, F.F.Tao. *Chem. Soc. Rev.*, **51**, 376 (2022); https://doi.org/10.1039/D1CS00783A
48. M.Ravi, M.Ranocchiari, J.A.Van Bokhoven. *Angew. Chem., Int. Ed.*, **56**, 16464 (2017); https://doi.org/10.1002/anie.201702550
49. H.Chen, A.Hu, L.Chang, Q.An, H.Pan, Zh.Zuo. In *The Chemical Transformations of C_1 Compounds: Direct Conversions of Methane via Homogeneous Processes*. (Eds X.F.Wu, B.Han, K.Ding, Zh.Liu). (Weinheim: Wiley-VCH, 2022). P. 1; https://doi.org/10.1002/9783527831883
50. Y.Chen, X.Mu, X.Luo, G.Yang, T.Wu. *Energy Technol.*, **8**, 1900750 (2020); https://doi.org/10.1002/ente.201900750
51. B.Li, X.Song, S.Feng, Q.Yuan, M.Jiang, L.Yan, Y.Ding. *Appl. Catal., B*, **293**, 120208 (2021); https://doi.org/10.1016/j.apcatb.2021.120208
52. J.J.Wen, Y.Xie, Y.P.Ma, H.Y.Sun, H.M.Wang, M.Liu, Q.L.Zhang, J.J.Chen. *Fuel*, **308**, 122008 (2022); https://doi.org/10.1016/j.fuel.2021.122008
53. R.Feng, P.Y.Niu, B.Hou, Q.Wang, L.T.Jia, M.G.Lin, D.B.Li. *J. Energy Chem.*, **67**, 342 (2022); https://doi.org/10.1016/j.jechem.2021.10.018
54. M.Torimoto, S.Ogo, D.Harjowinoto, T.Higo, J.G.Seo, S.Furukawa, Y.Sekine.*Chem. Commun.*, **55**, 6693 (2019); https://doi.org/10.1039/C9CC02794G
55. V.Fung, G.X.Hu, B.Sumpter. *J. Mater. Chem. A*, **8**, 6057 (2020); https://doi.org/10.1039/D0TA00375A
56. D.M.Zakharov, N.A.Zhuravlev, T.A.Denisova, A.S.Belozerov, A.Y.Stroeva, E.G.Vovkotrub, A.S.Farlenkov, M.V.Ananyev. *J. Catal.*, **394**, 67 (2021); https://doi.org/10.1016/j.jcat.2020.12.011
57. M.V.Ananyev, D.M.Zakharov. *Catal. Sci. Technol.*, **10**, 3561 (2020); https://doi.org/10.1039/C9CY02566A
58. R.Feng, P.Y.Niu, Q.Wang, B.Hou, L.T.Jia, M.G.Lin, D.B.Li. *Fuel*, **308**, 121848 (2022); https://doi.org/10.1016/j.fuel.2021.121848
59. Y.X.Zhao, Z.Y.Li, S.G.He. *Acc. Chem. Res.*, **51**, 2603 (2018); https://doi.org/10.1021/acs.accounts.8b00403
60. Y.Fan, Y.Yue, W.Hua, Z.Gao, Ch.Miao. *Reac. Kinet. Mechan. Catal.*, **134**, 711 (2021); https://doi.org/10.1007/s11144-021-02085-7
61. X.J.Cui, H.B.Li, Y.Wang, Y.L.Hu, L.Hua, H.Y.Li, X.W.Han, Q.F.Liu, F.Yang, L.M.He, X.Q.Chen, Q.Li, J.Xiao, D.Deng, X.Bao. *Chem.*, **4**, 1902 (2018); https://doi.org/10.1016/j.chempr.2018.05.006
62. J.Xu, A.M.Zheng, X.M.Wang, G.D.Qi, J.H.Su, J.F.Du, Z.H.Gan, J.F.Wu, W.Wang, F.Deng. *Chem. Sci.*, **3**, 2932 (2012); https://doi.org/10.1039/c2sc20434g
63. Y.Shi, Y.Zhou, Y.Lou, Z.Chen, H.Xiong, Y.Zhu. *Adv. Sci.*, **9**, 2201520 (2022); https://doi.org/10.1002/ad*vs*.202201520
64. T.Yu, Zh.Li, L.Lin, Sh.Chu, Y.Su, W.Song, A.Wang, B.M.Weckhuysen, W.Luo. *ACS Catal.*, **11**, 6684 (2021); https://doi.org/10.1021/acscatal.1c00905
65. L.Zhang, J.Zhu, X.Li, Sh.Mu, F.Verpoort, J.Xue, Z.Kou, J.Wang. *Interdiscip Mater.*, **1**, 51 (2022); https://doi.org/10.1002/idm2.12011
66. Ch.Ye, N.Zhang, D.Wang, Y.Li. *Chem. Commun.*, **56**, 7687 (2020); https://doi.org/10.1039/D0CC03221B
67. Sh.Ji, Y.Chen, X.Wang, Z.Zhang, D.Wang, Y.Li. *Chem. Rev.*, **120**, 11900 (2020); https://doi.org/10.1021/acs.chemrev.9b00818
68. E.Le Saché, T.R.Reina. *Prog. Energy Combust. Sci.*, **89**, 100970 https://doi.org/10.1016/j.pecs.2021.100970 (2022)
69. M.Babucci, A.Guntida, B.C.Gates. *Chem. Rev.*, **120**, 11956 (2020); https://doi.org/10.1021/acs.chemrev.0c00864
70. N.H.M.Dostagir, R.Rattanawan, M.Gao, J.Ota, J.Y.Hasegawa, K.Asakura, A.Fukouka, A.Shrotri. *ACS Catal.*, **11**, 9450 (2021); https://doi.org/10.1021/acscatal.1c02041
71. L.Li, X.Chang, X.Lin, Zh.J.Zhao, J.Gong. *Chem. Soc. Rev.*, **49**, 8156 (2020); https://doi.org/10.1039/D0CS00795A
72. L.C.Liu, A.Corma. *Chem.*, **7**, 2347 (2021); https://doi.org/10.1021/acsnano.0c06610
73. H.Jeong, S.Shin, H.Lee. *ACS Nano*, **14**, 14355 (2020); https://doi.org/10.1021/acsnano.0c06610
74. S.H.Wang, H.B.Li, M.Q.He, X.J.Cui, L.Hua, H.Y.Li, J.P.Xiao, L.Yu, N.P.Rajan, Z.X.Xie, D.Deng. *J. Energy Chem.*, **36**, 47 (2019); https://doi.org/10.1016/j.jechem.2019.04.003
75. T.Zhang, X.W.Nie, W.W.Yu, X.W.Guo, C.S.Song, R.Si, Y.F.Liu, Z.K.Zhao. *Science*, **22**, 97 (2019); https://doi.org/10.1016/j.isci.2019.11.010
76. W.L.Zhu, J.J.Fu, J.Liu, Y.Chen, X.Li, K.K.Huang, Y.M.Cai, Y.M.He, Y.Zhou, D.Su,J.J.Zhu, Y.Lin. *Appl. Catal. B*, **264**, 118502 (2020); https://doi.org/10.1016/j.apcatb.2019.118502
77. A.Wang, J.Li, T.Zhang. *Nat. Rev. Chem.*, **2**, 65 (2018); https://doi.org/10.1038/s41570-018-0010-1
78. G.Q.Fang, J.Lin, X.D.Wang. *Chin. J. Chem. Eng.*, **38**, 18 (2021); https://doi.org/10.1016/j.cjche.2021.04.034
79. Q.Zhang, J.Guan. *Adv. Functional Mater.*, **30**, 2000768 (2020); https://doi.org/10.1002/adfm.202000768
80. K.K.Irikura. *J. Chem. Phys.*, **154**, 174302 (2021); https://doi.org/10.1063/5.0044996
81. Ph.Serp. *Nanoscale*, **13**, 5985 (2021); https://doi.org/10.1039/D1NR00465D
82. R.Qin, K.Liu, Q.Wu,N.Zheng. *Chem. Rev.*, **120**, 11810 (2020); https://doi.org/10.1021/acs.chemrev.0c00094
83. W.Zhang, Q.Fu, Q.Luo, L.Sheng, J.Yang. *J. Am. Chem. Soc. Au*, **1**, 2130 (2021); https://doi.org/10.1021/jacsau.1c00384
84. J.Liu. *Curr. Opin. Green Sust. Chem.*, **22**, 54 (2020); https://doi.org/10.1016/j.cogsc.2020.01.004
85. S.K.Kaiser, Z.Chen, D.F.Akl, Sh.Mitchell, J.Pérez-Ramírez. *Chem. Rev.*, **120**, 11703 (2020); https://doi.org/10.1021/acs.chemrev.0c00576
86. Z.Kou, W.Zang, P.Wang, X.Li,J.Wang. *Nanoscale Horiz.*, **5**, 757 (2020); https://doi.org/10.1039/D0NH00088D
87. R.Lang, X.Du, Y.Huang, X.Jiang, Q.Zhang, Y.Guo, K.Liu, B.Qiao, A.Wang,T.Zhang. *Chem. Rev.*, **120**, 11986 (2020); https://doi.org/10.1021/acs.chemrev.0c00797
88. R.Li, L.Luo, X.Ma, W.Wu, M.Wang, J.Zeng. *J. Mater. Chem. A*, **10**, 5717 (2022); https://doi.org/10.1039/D1TA08016D

89. C.Du, H.Lin, B.Lin, Z.Ma, T.Hou, J.Tang, Y.Li. *J. Mater. Chem. A*, **3**, 23113 (2015); https://doi.org/10.1039/C5TA05084G
90. F.Kraushofer, G.S.Parkinson. *Chem. Rev.*, **122**, 14911 (2022); https://doi.org/10.1021/acs.chemrev.2c00259
91. J.Kim, H.E.Kim, H.Lee.*ChemSusChem.*, **1**, 104 (2017); https://doi.org/10.1002/cssc.201701306
92. X.M.Cao, H.J.Zhou, L.Y.Zhao, X.N.Chen, P.J.Hu. *Chin. Chem. Lett.*, **32**, 1972 (2021); https://doi.org/10.1016/j.cclet.2020.09.015
93. H.E.Kim, I.H.Lee, J.Cho, S.Shin, H.Ch.Ham, J.Y.Kim, H.Lee. *ChemElectroChem.*, **6**, 4757 (2019); https://doi.org/10.1002/celc.201900772
94. S.Shin, H.E.Kim, B.S.Kim, S.Seo, J.H.Jeong,H.Lee. *ChemElectroChem.*, **7**, 3716 (2020); https://doi.org/10.1002/celc.202000926
95. C.Kirk, L.D.C.Section, S.Siahrostami, M.Karamad, M.Bajdich, J.Voss, J.K.Norskov, K.Chan. *ACS Central Sci.*, **3**, 1286 (2017); https://doi.org/10.1021/acscentsci.7b00442
96. X.Su, X.F.Yang, Y.Q.Huang, B.Liu, T.Zhang. *Acc. Chem. Res.*, **52**, 656 (2019); https://doi.org/10.1021/acs.accounts.8b00478
97. T.Zhang, Z.Chen, A.G.Walsh, Y.Li, P.Zhang. *Adv. Mater.*, **32**, 2002910 (2020); https://doi.org/10.1002/adma.202002910
98. S.Chen, M.Cui, Z.Yin, J.Xiong, L.Mi, Y.Li. *ChemSusChem*, **14**, 73 (2021); https://doi.org/10.1002/cssc.202002098
99. Y.Deng, P.Tian, Sh.Liu, H.He, Y.Wang, L.Ouyang, Sh.Yuan. *J. Hazard. Mater.*, **426**, 127793 (2022); https://doi.org/10.1016/j.jhazmat.2021.127793
100. S.Zhang, L.Nguyen, J.X.Liang, J.Shan, J.J.Liu, A.I.Frenkel, A.Patlolla, W.Huang, J.Li, F.Tao. *Nat. Commun.*, **6**, 7938 (2015); https://doi.org/10.1038/ ncomms8938
101. B.Zhang, T.Fan, N.Xie, G.Nie, H.Zhang. *Adv. Sci.*, **6**, 1901787 (2019); https://doi.org/10.1002/ad*vs*.201901787
102. P.Liu, Y.Zhao, R.Qin, S.Mo, G.Chen, L.Gu, D.M.Chevrier, P.Zhang, Q.Guo, D.Zang, B.Wu, G.Fu, N.Zheng. *Science*, **352**, 797 (2016); https://doi.org/10.1126/science.aaf5251
103. M.K.Samantaray, V.D'Elia, E.Pump, L.Falivene, M.Harb, S.O.Chikh, L.Cavallo, J.M.Basset. *Chem. Rev.*, **120**, 734 (2020); https://doi.org/10.1021/acs.chemrev.9b00238
104. Q.Zhang, J.Guan. *Nano Res.*, **15**, 38 (2022); https://doi.org/10.1007/s12274-021-3479-8
105. R.T.Hannagan, G.Giannakakis, M.Flytzani-Stephanopoulos, E.Ch.H.Sykes. *Chem. Rev.*, **120**, 12044 (2020); https://doi.org/10.1021/acs.chemrev.0c00078
106. Z.Chen, P.Zhang. *ACS Omega*, **7**, 1585 (2022); https://doi.org/10.1021/acsomega.1c06067
107. Zh.Xu, Zh.Ao, M.Yang, Sh.Wang. *J. Hazard. Mater.*, **424**, 127427 (2022); https://doi.org/10.1016/j.jhazmat.2021.127427
108. W.Zhou, H.Su, Z.Wang, F.Yu, W.Wang, X.Chen, Q.Liu. *J. Mater. Chem. A*, **9**, 1127 (2021); https://doi.org/10.1039/D0TA10267A
109. Z.Liu, S.Zhou, S.Ma, J.Li, Z.Yang, H.Cheng, W.Cai. *Mater. Today Phys.*, **17**, 100338 (2021); https://doi.org/10.1016/j.mtphys.2020.100338
110. Y.Ma, T.Yang, H.Zou, W.Zang, Z.Kou, L.Mao, Y.Feng, L.Shen, S.J.Pennycook, L.Duan, X.Li, J.Wang. *Adv. Mater.*, **32**, 2002177 (2020); https://doi.org/10.1002/adma.202002177
111. Sh.Mitchell, J.Pérez-Ramírez. *Nat. Commun.*, **11**, 4302 (2020); https://doi.org/10.1038/s41467-020-18182-5
112. H.Xiong, A.K.Datye, Y.Wang. *Adv. Mater.*, **33**, 2004319 (2021); https://doi.org/10.1002/adma.202004319
113. H.Xu, Y.Zhao, Q.Wang, G.He, H.Chen. *Coord. Chem. Rev.*, **451**, 214261 (2022); https://doi.org/10.1016/j.ccr.2021.214261
114. Y.Mu, T.Wang, J.Zhang, Ch.Meng, Y.Zhang, Z.Kou. *Electrochem. Energy Rev.*, **5**, 145 (2022); https://doi.org/10.1007/s41918-021-00124-4
115. Y.Zhao, W.J.Jiang, J.Zhang, E.C.Lovell, R.Amal, Zh.Han, X.Lu. *Adv. Mater.*, **33**, 2102801 (2021); https://doi.org/10.1002/adma.202102801
116. L.Zhang, Y.Shi, L.Li, L.Wang, J.L.Han, A.J.Wang. *Electrochem. Sci. Adv.*, **2**, e202100102 (2022); https://doi.org/10.1002/elsa.202100102
117. Q.Zuo, T.Liu, C.Chen, Y.Ji, X.Gong, Y.Mai, Y.Zhou. *Angew. Chem., Int. Ed.*, **58**, 10198 (2019); https://doi.org/10.1002/anie.201904058
118. Y.Chen, S.Ji, W.Sun, Y.Lei, Q.Wang, A.Li, W.Chen, G.Zhou, Z.Zhang, Y.Wang, L.Zheng, Q.Zhang, L.Gu, X.Han, D.Wang, Y.Li. *Angew. Chem., Int. Ed.*, **59**, 1295 (2020); https://doi.org/10.1002/anie.201912439
119. Q.Ma, W.Zhang, J.Young. *Surf. Sci.*, **715**, 121949 (2022); https://doi.org/10.1016/j.susc.2021.121949
120. L.Chen, Zh.Qi, Sh.Zhang, J.Su, G.A.Somorjai. *Trends Chem.*, **2**, 1114 (2020); https://doi.org/10.1016/j.trechm.2020.09.009
121. Sh.Ding, M.J.Hülsey, J.Pérez-Ramírez, N.Yan. *Joule*, **3**, 2897 (2019); https://doi.org/10.1016/j.joule.2019.09.015
122. T.Cui, L.Li, Ch. Ye, X.Li, Ch.Liu, Sh.Zhu, W.Chen, D.Wang. *Adv. Funct. Mater.*, **32**, 2108381 (2021); https://doi.org/10.1002/adfm.202108381
123. B.Singh, V.Sharma, R.P.Gaikwad, P.Fornasiero, R.Zbořil, M.B.Gawande. *Nano Micro Small*, **17**, 2006473 (2021); https://doi.org/10.1002/smll.202006473
124. B.B.Sarma, Ph.N.Plessow, G.Agostini, P.Concepción, N.Pfänder, L.Kang, F.R.Wang, F.Studt, G.Prieto. *J. Am. Chem. Soc.*, **142**, 14890 (2020); https://doi.org/10.1021/jacs.0c03627
125. P.Kumar, T.A.Al-Attas, J.Hu, M.G.Kibria. *ACS Nano*, **16**, 8557 (2022); https://doi.org/10.1021/acsnano.2c02464
126. Y.Liu, R.Wang, Ch.K.Russell, P.Jia, Y.Yao, W.Huang, M.Radosz, Kh.A.M.Gasem, H.Adidharma, M.Fan. *Coord. Chem. Rev.*, **470**, 214691 (2022); https://doi.org/10.1016/j.ccr.2022.214691
127. S.Kim, J.Lauterbach, E.Sasmaz. *ACS Catal.*, **11**, 8247 (2021); https://doi.org/10.1021/acscatal.1c01223
128. M.Akri, A.E.Kasmi, C.Batiot-Dupeyrat, B.Qiao. *Catalysts*, **10**, 630 (2020); https://doi.org/10.3390/catal10060630
129. S.Sorcar, J.Das, E.P.Komarala, L.Fadeev, B.A.Rosen, M.Gozin. *Mater. Today Chem.*, **24**, 100765 (2022); https://doi.org/10.1016/j.mtchem.2021.100765
130. P.G.Lustemberg, Zh.Mao, A.Salcedo, B.Irigoyen, M.V.Ganduglia-Pirovano, Ch.T.Campbel. *ACS Catal.*, **11**, 10604 (2021); https://doi.org/10.1021/acscatal.1c02154
131. Y.B.Wang, L.He, B.Ch.Zhou, F.Tang, J.Fan, D.Q.Wang, A.H.Lu, W.C.Li. *Ind. Eng. Chem. Res.*, **60**, 15064 (2021); https://doi.org/10.1021/acs.iecr.1c02895
132. K.Nakamura, K.Okumura, E.Tsuji, S.Suganuma, N.Katada. *ChemCatChem.*, **12**, 2333 (2020); https://doi.org/10.1002/cctc.202000030
133. K.Nakamura, A.Okuda, K.Ohta, H.Matsubara, K.Okumura, K.Yamamoto, R.Itagaki, S.Suganuma, E.Tsuji, N.Katada. *ChemCatChem.*, **10**, 3806 (2018); https://doi.org/10.1002/cctc.201800724
134. H.Matsubara, E.Tsuji, Y.Moriwaki, K.Okumura, K.Yamamoto, K.Nakamura, S.Suganuma, N.Katada. *Catal. Lett.*, **149**, 2627 (2019); https://doi.org/10.1007/s10562-019-02855-y
135. P.Hu, K.Nakamura, H.Matsubara, K.Iyoki, Y.Yanaba, K.Okumura, T.Okubo, N.Katada, T.Wakihara. *Appl. Catal. A*, **601**, 117661 (2020); https://doi.org/10.1016/j.apcata.2020.117661
136. H.Wang, W.Xin, Q.Wang, X.Zheng, Z.Lu, R.Pei, P.He, X.Dong. *Catal. Commun.*, **162**, 106374 (2022); https://doi.org/10.1016/j.catcom.2021.106374
137. S.Sogukkanli, T.Moteki, M.Ogura. *Green Chem.*, **23**, 2148 (2021); https://doi.org/10.1039/D0GC03645E
138. M.Li, J.Shan, G.Giannakakis, M.Ouyang, S.Cao, S.Lee, L.F.Allard, M.Flytzani-Stephanopoulos. *Appl. Catal. B*, **292**, 120124 (2021); https://doi.org/10.1016/j.apcatb.2021.120124
139. R.Shavi, J.Ko, A.Cho, J.W.Han, J.G.Seo. *Appl. Catal. B*, **229**, 237 (2018); https://doi.org/10.1016/j.apcatb.2018.01.058

140. Y.Li, B.Liu, J.Liu, T.Wang, Y.Shen, K.Zheng, F.Jiang, Y.Xu, X.Liu. *New J. Chem.*, **45**, 8978 (2021); https://doi.org/10.1039/D1NJ00794Ghttps://doi.org/10.1039/D1NJ00794G
141. T.Ban, X.Y.Yu,H.Zh.Kang, H.X.Zhang, X.Gao, Zh.Q.Huang, Ch.R.Chang. *J. Catal.*, **408**, 206 (2022); https://doi.org/10.1016/j.jcat.2022.03.004
142. Y.Zhao, H.Wang, J.Han, X.Zhu, D.Mei, Q.Ge. *ACS Catal.*, **9**, 3187 (2019); https://doi.org/10.1021/acscatal.9b00291
143. X.Nie, X.Ren, Ch.Tu, Ch.Song, X.Guo, J.G.Chen. *Chem. Commun.*, **56**, 3983 (2020); https://doi.org/10.1039/C9CC10055E
144. Y.Kwon, T.Kim, G.Kwon, J.Yi, H.Lee. *J. Am. Chem. Soc.*, **139**, 17694 (2017); https://doi.org/10.1021/jacs.7b11010
145. K.Dutta, M.Shahryari, J.Kopyscinski. *Ind. Eng. Chem. Res.*, **59**, 4245 (2020); https://doi.org/10.1021/acs.iecr.9b05548
146. D.Bajec, A.Kostyniuk, A.Pohar, B.Likozar. *Chem. Eng. J.*, **396**, 125182 (2020); https://doi.org/10.1016/j.cej.2020.125182
147. H.X.Liu, T.Ban, X.Y.Yu, Zh.Q.Huang, Ch.R.Chang. *J. Phys. Chem. C*, **125**, 23212 (2021); https://doi.org/10.1021/acs.jpcc.1c07583
148. C.Xu, Q.Song, N.Merdanoglu, H.Liu, E.Klemm. *Methane*, **1**, 107 (2022); https://doi.org/10.3390/methane1020010
149. S.Hong, G.Mpourmpakis. *Catal. Sci. Technol.*, **11**, 6390 (2021); https://doi.org/10.1039/D1CY00826A
150. X.Tang, L.Wang, B.Yang, Ch.Fei, T.Yao, W.Liu, Y.Lou, Q.Dai, Y.Cai, X.M.Cao, W.Zhan, Y.Guo, X.Q.Gong, Y.Guo. *Appl. Catal. B*, **285**, 119827 (2021); https://doi.org/10.1016/j.apcatb.2020.119827
151. X.Yu, L.Zhong, Sh.Li. *Phys. Chem. Phys. Chem.*, **23**, 4963 (2021); https://doi.org/10.1039/D0CP06696F
152. R.F.Chen, W.S.Xia, H.L.Wan. *Chem. J. Chin. Univ.-Chin.*, **36**, 1743 (2015); https://doi.org/10.7503/cjcu20150218
153. F.S.Liu, W.Chu, W.J.Sun, Y.Xue, Q.Jiang. *J. Nat. Gas Chem.*, **21**, 708 (2012); https://doi.org/10.1016/S1003-9953(11)60423-4
154. M.C.Cholewins, M.Dixit, G.Mpourmpakis. *ACS Omega*, **3**, 18242 (2018); https://doi.org/10.1021/acsomega.8b02554
155. T.Kreuger, W.P.M.Van Swaaij, A.N.R.Bos, S.R.A.Kersten. *Chem. Eng. J.*, **427**, 130412 (2022); https://doi.org/10.1016/j.cej.2021.130412
156. G.S.Liu, W.Q.Huang, Y.Li, K.N.Ding, W.K.Chen, Y.F.Zhang, W.Lin. *Appl. Surf. Sci.*, **555**, 149728 (2021); https://doi.org/10.1016/j.apsusc.2021.149728
157. Y.Wang, L.Y.Zhao, L.Shi, J.Sheng, W.P.Zhang, X.M.Cao, P.J.Hu, A.H.Lu. *Catal. Sci. Technol.*, **8**, 2051 (2018); https://doi.org/10.1039/C8CY00163D
158. S.Raynes, M.A.Shah, R.A.Taylor. *Dalton Trans.*, **48**, 10364 (2019); https://doi.org/10.1039/C9DT00922A
159. P.Del Campo, C.Martínez, A.Corma. *Chem. Soc. Rev.*, **50**, 8511 (2021); https://doi.org/10.1039/D0CS01459A
160. X.L.Zhao, J.Xu, Y.Y.Chu, G.D.Qi, Q.Wang, W.Gao, S.H.Li, N.D.Feng, F.Dang. *ChemCatChem.*, **12**, 3880 (2020); https://doi.org/10.1002/cctc.202000650
161. Z.R.Jovanovic, J.P.Lange, M.Ravi, A.J.Knorpp, V.L.Sushkevich, M.A.Newton, D.Palagin, J.A.Van Bokhoven. *J. Catal.*, **385**, 238 (2020); https://doi.org/10.1016/j.jcat.2020.02.001
162. O.Adeyiga, O.Suleiman, S.O.Odoh. *Inorg. Chem.*, **60**, 8489 (2021); https://doi.org/10.1021/acs.inorgchem.0c03510
163. H.Zhang, Y.G.Ji, Y.Xu, P.Deng, J.Li, Y.Lei, J.Yang, X.Tian. *Mater. Today Sustainability*, **22**, 100351 (2023); https://doi.org/10.1016/j.mtsust.2023.100351
164. J.Zheng, J.Y.Ye, M.A.Ortuno, J.L.Fulton, O.Y.Gutierrez, D.M.Camaioni, R.K.Motkuri, Z.Y.Li, T.E.Webber, B.L.Mehdi, N.D.Browning, R.L.Penn, O.K.Farha, J.T.Hupp, D.G.Truhlar, Ch.J.Cramer, J.A.Lerche. *J. Am. Chem. Soc.*, **141**, 9292 (2019); https://doi.org/10.1021/jacs.9b02902
165. N.Kuriakose, U.Mondal, P.Ghosh. *J. Mater. Chem. A*, **9**, 23703 (2021); https://doi.org/10.1039/D1TA00626F
166. H.Prats, R.A.Gutiérrez, J.J.Piñero, F.Viñes, S.T.Bromley, P.J.Ramírez, J.A.Rodriguez, F.Illas. *J. Am. Chem. Soc.*, **141**, 5303 (2019); https://doi.org/10.1021/jacs.8b13552
167. Q.Chen, Y.X.Zhao, J.J.Chen, L.X.Jiang, S.G.He. *Zh. Phys. Chem.*, **233**, 785 (2019); https://doi.org/10.1515/zpch-2018-1334
168. Q.Chen, Y.X.Zhao, L.X.Jiang, H.F.Li, J.J.Chen, T.Zhang, Q.Y.Liu, S.G.He. *Phys. Chem. Chem. Phys.*, **20**, 4641 (2018); https://doi.org/10.1039/C8CP00071A
169. Y.Shen, Q.Du, Y.Zhao, S.Zhou, J.Zha. *Chem. Phys. Lett.*, **779**, 138829 (2021); https://doi.org/10.1016/j.cplett.2021.138829
170. S.D.Zhao, L.S.Ma, Y.Y.Xi, H.Y.Shang, X.F.Lin. *RSC Adv.*, **11**, 11295 (2021); https://doi.org/10.1039/D0RA10785A
171. S.D.Zhou, X.Y.Sun, L.Yue, M.Schlangen. *Int. J. Mass Spectr.*, **434**, 240 (2018); https://doi.org/10.1016/j.ijms.2018.10.009
172. B.Yuan, Sh.Y.Tang, Sh.Zhou. *Chem. A Eur. J.*, **28**, e202201136 (2022); https://doi.org/10.1002/chem.202201136
173. G.Yan, Z.Y.Gao, M.L.Zhao, K.Ma, Z.Ding, W.J.Yang, X.L.Ding. *Mol. Catal.*, **497**, 111205 (2020); https://doi.org/10.1016/j.mcat.2020.111205
174. J.Sirijaraensre, J.Limtrakul. *Phys. Chem. Chem. Phys.*, **17**, 9706 (2015); https://doi.org/10.1039/C4CP05131A
175. J.G.Polynskaya, A.V.Lebedev, A.A.Knizhnik, A.S.Sinitsa, R.V.Smirnov, B.V.Potapkin. *Comput. Theor. Chem.*, **1147**, 51 (2019); https://doi.org/10.1016/j.comptc.2018.12.006
176. Y.Ren, Y.Yang, Y.X.Zhao, Sh.G.He. *J. Phys. Chem. C*, **123**, 17035 (2019); https://doi.org/10.1021/acs.jpcc.9b04750
177. J.F.Eckhard, T.Masubuchi, M.Tschurl, R.N.Barnett, U.Landman, U.Heiz. *J. Phys. Chem A*, **125**, 5289 (2021); https://doi.org/10.1021/acs.jpca.1c02384
178. P.G.Lustemberg, F.Zhang, R.A.Gutiérrez, P.J.Ramírez, S.D.Senanayake, J.A.Rodriguez, M.V.Ganduglia-Pirovano. *J. Phys. Chem. Lett.*, **11**, 9131 (2020); https://doi.org/10.1021/acs.jpclett.0c02109
179. V.Fung, F.Tao, D.E.Jiang. *Phys. Chem. Chem. Phys.*, **20**, 22909 (2018); https://doi.org/10.1039/C8CP03191F
180. F.Zhang, R.A.Gutiérrez, P.G.Lustemberg, Z.Liu, N.Rui, T.Wu, P.J.Ramírez, W.Xu, H.Idriss, M.V.Ganduglia-Pirovano, S.D.Senanayake, J.A.Rodriguez. *ACS Catal.*, **11**, 1613 (2021); https://doi.org/10.1021/acscatal.0c04694
181. Y.Ren, Y.Yang, Y.X.Zhao, Sh.G.He. *J. Am. Chem. Soc. Au*, **2**, 197 (2022); https://doi.org/10.1021/jacsau.1c00469
182. M.M.Wang, Y.X.Zhao, X.L.Ding, W.Li, Sh.G.He. *Phys. Chem. Chem. Phys.*, **22**, 6231 (2020); https://doi.org/10.1039/C9CP05699H
183. Y.K.Li, Y.X.Zhao, Sh.G.He. *J. Phys. Chem. A*, **122**, 3950 (2018); https://doi.org/10.1021/acs.jpca.8b02483
184. Y.Yang, Y.K.Li, Y.X.Zhao, G.P.Wei, Y.Ren, K.R.Asmis, Sh.G.He. *Angew. Chem., Int. Ed.*, **60**, 13788 (2021); https://doi.org/10.1002/anie.202103808
185. K.Koszinowski, M.Schlangen, D.Schröder, H.Schwarz. *Int. J. Mass Spectrom.*, **237**, 19 (2004); https://doi.org/10.1016/j.ijms.2004.06.009
186. D.J.Harding, Ch.Kerpal, G.Meijer, A.Fielicke. *Angew. Chem., Int. Ed.*, **51**, 817 (2012); https://doi.org/10.1002/anie.201107042
187. G.Liu, Z.Zhu, S.M.Ciborowski, I.R.Ariyarathna, E.Miliordos, K.H.Bowen. *Angew. Chem. Int. Ed.*, **58**, 7773 (2019); https://doi.org/10.1002/anie.201903252
188. G.Liu, I.R.Ariyarathna, S.M.Ciborowski, Zh.Zhu, E.Miliordos, K.H.Bowen. *J. Am. Chem. Soc.*, **142**, 21556 (2020); https://doi.org/10.1021/jacs.0c11112
189. S.M.Lang, A.Frank, Th.M.Bernhardt. *J. Phys. Chem. C*, **117**, 9791 (2013); https://doi.org/10.1021/jp312852r
190. S.M.Lang, T.M.Bernhardt, R.N.Barnett, U.Landman. *Angew. Chem., Int. Ed.*, **49**, 980 (2010); https://doi.org/10.1002/anie.200905643
191. S.M.Lang, T.M.Bernhardt, V.Chernyy, J.M.Bakker, R.N.Barnett, U.Landman. *Angew. Chem., Int. Ed.*, **56**, 13406 (2017); https://doi.org/10.1002/anie.201706009

192. M.Citir, F.Liu, P.B.Armentrout. *J. Chem. Phys.*, **130**, 054309 (2009); https://doi.org/10.1063/1.3073886
193. F.Liu, X.G.Zhang, R.Liyanage, P.B.Armentrout. *J. Chem. Phys.*, **121**, 10976 (2004); https://doi.org/10.1063/1.1814095
194. C.W.Copeland, M.A.Ashraf, E.M.Boyle, R.B.Metz. *J. Phys. Chem. A*, **121**, 2132 (2017); https://doi.org/10.1021/acs.jpca.6b13074
195. P.B.Armentrout, M.R.Sievers. *J. Phys. Chem. A*, **107**, 4396 (2003); https://doi.org/10.1021/jp027820d
196. S.M.Lang, A.Frank, T.M.Bernhardt. *Int. J. Mass Spectrom.*, **354**–**355**, 365 (2013); https://doi.org/10.1016/j.ijms.2013.07.014
197. K.Koszinowski, D.Schröder, H.Schwarz. *ChemPhysChem.*, **4**, 1233 (2003); https://doi.org/10.1002/cphc.200300840
198. P.B.Armentrout. *Chem. – Eur. J.*, **23**, 10 (2017); https://doi.org/10.1002/chem.201602015
199. V.J.F.Lapoutre, B.Redlich, A.F.G.Van der Meer, J.Oomens, J.M.Bakker, A.Sweeney, A.Mookherjee, P.B.Armentrout. *J. Phys. Chem. A*, **117**, 4115 (2013); https://doi.org/10.1021/jp400305k
200. N.Levin, J.Lengyel, J.F.Eckhard, M.Tschurl, U.Heiz. *J. Am. Chem. Soc.*, **142**, 5862 (2020); https://doi.org/10.1021/jacs.0c01306
201. H.Schwarz, S.Shaik, J.Li. *J. Am. Chem. Soc.*, **139**, 17201 (2017); https://doi.org/10.1021/jacs.7b10139
202. S.Bai, F.Liu, B.Huang, F.Li, H.Lin, T.Wu, M.Sun, J.Wu, Q.Shao,Y.Xu, X.Huang. *Nat. Commun.*, **11**, 954 (2020); https://doi.org/10.1038/s41467-020-14742-x
203. Y.Q.Su, J.X.Liu, I.A.W.Filot, L.Zhang, E.J.M.Hensen. *ACS Catal.*, **8**, 6552 (2018); https://doi.org/10.1021/acscatal.8b01477
204. M.Chabanas, V.Vidal, C.Coperet, J.Thivolle-Cazat, J.M.Basset. *Angew. Chem., Int. Ed.*, **39**, 1962 (2000); https://doi.org/10.1002/1521-3773(20000602)39:11<1962::AID-ANIE1962>3.0.CO;2-1
205. Ch.Wu, I.D.Gates. *Mol. Catal.*, **469**, 40 (2019); https://doi.org/10.1016/j.mcat.2019.03.002
206. C.Choi, S.Yoon, Y.Jung. *Chem. Sci.*, **12**, 3551 (2021); https://doi.org/10.1039/D0SC05632D
207. G.Qi,Q.Wang, J.Xu, J.Trébosc, O.Lafon, Ch.Wang, J.P.Amoureux, F.Deng. *Angew. Chem., Int. Ed.*, **128**, 16058 (2016); https://doi.org/10.1002/ange.201608322
208. Y.J.Xi, A.Heyden. *J. Catal.*, **386**, 12 (2020); https://doi.org/10.1016/j.jcat.2020.03.036
209. Q.Shen, C.Cao, R.Huang, L.Zhu, X.Zhou, Q.Zhang, L.Gu, W.Song. *Angew. Chem., Int. Ed.*, **59**, 1216 (2020); https://doi.org/10.1002/anie.201913309
210. V.Fung, G.Hu, F.F.Tao, D.Jiang. *ChemPhysChem.*, **20**, 2217 (2019); https://doi.org/10.1002/cphc.201900497
211. Q.Wan, V.Fung, S.Lin, Z.Wu, D.Jiang. *J. Mater. Chem. A*, **8**, 4362 (2020); https://doi.org/10.1039/C9TA11712A
212. J.Shan, M.Li, L.F.Allard, S.Lee, M.Flytzani-Stephanopoulos. *Nature (London)*, **551**, 605 (2017); https://doi.org/10.1038/nature24640
213. K.Harrath, X.Yu, H.Xiao, J.Li. *ACS Catal.*, **9**, 8903 (2019); https://doi.org/10.1021/acscatal.9b02093
214. J.H.Wen, D.Guo, G.Ch.Wang. *Appl. Surf. Sci.*, **555**, 149690 (2021); https://doi.org/10.1016/j.apsusc.2021.149690
215. G.Righi, R.Magri, A.Selloni. *J. Phys. Chem. C*, **124**, 17578 (2020); https://doi.org/10.1021/acs.jpcc.0c03320
216. M.Akri, S.Zhao, X.Li, K.Zang, A.F.Lee, M.A.Isaacs, W.Xi, Y.Gangarajula, J.Luo, Y.Ren, Y.T.Cui, L.Li, Y.Su, X.Pan, W.Wen, Y.Pan, K.Wilson, L.Li, B.Qiao, H.Ishii, Y.F.Liao, A.Wang, X.Wang, T.Zhang. *Nat. Commun.*, **10**, 5181 (2019); https://doi.org/10.1038/s41467-019-12843-w
217. Y.Tang, Y.Wei, Z.Wang, S.Zhang, Y.Li, L.Nguyen, Y.Li, Y.Zhou, W.Shen, F.F.Tao, P.Hu. *J.Am. Chem. Soc.*, **141**, 7283 (2019); https://doi.org/10.1021/jacs.8b10910
218. Y.Zhao, C.Cui, J.Han, H.Wang, X.Zhu, Q.Ge. *J. Am. Chem. Soc.*, **138**, 10191 (2016); https://doi.org/10.1021/jacs.6b04446
219. R.J.Bunting, J.Thompson, P.Hu. *Phys. Chem. Chem. Phys.*, **22**, 11686 (2020); https://doi.org/10.1039/D0CP01284J
220. T.Moteki, N.Tominaga, M.Ogura. *Appl. Catal. B*, **300**, 120742 (2022); https://doi.org/10.1016/j.apcatb.2021.120742
221. T.Moteki, N.Tominaga, N.Tsunoji, T.Yokoi, M.Ogura. *Chem. Lett.*, **50**, 1597 (2021); https://doi.org/10.1246/cl.210250
222. Y.Hou, Sh.Nagamatsu, K.Asakura, A.Fukuoka, H.Kobayashi. *Commun. Chem.*, **1**, 41 (2018); https://doi.org/10.1038/s42004-018-0044-9
223. W.X.Huang, S.R.Zhang, Y.Tang, Y.T.Li, L.Nguyen, Y.Y.Li, J.J.Shan, D.Q.Xiao, R.Gagne, A.I.Frenkel, F.F.Tao. *Angew. Chem., Int. Ed.*, **55**, 13441 (2016); https://doi:org/10.1002/anie.201604708
224. A.A.Gabrienko, S.A.Yashnik, A.A.Kolganov, A.M.Sheveleva, S.S.Arzumanov, M.V.Fedin, F.Tuna, A.G.Stepanov. *Inorg. Chem.*, **59**, 2037 (2020); https://doi.org/10.1021/acs.inorgchem.9b03462
225. A.Szecsenyi, G.N.Li, J.Gascon, E.A.Pidko. *ACS Catal.*, **8**, 7961 (2018); https://doi.org/10.1021/acscatal.8b01672
226. T.Yu, Z.Li, W.Jones, Y.S.Liu, Q.He, W.Y.Song, P.F.Du, B.Yang, H.Y.An, D.M.Farmer, C.W.Qiu, A.Q.Wang, B.M.Weckhuysen, A.M.Beale, W.H. Luo. *Chem. Sci.*, **12**, 3152 (2021); https://doi.org/10.1039/D0SC06067D
227. J.F.Wu, S.M.Yu, W.D.Wang, Y.X.Fan, S.Bai, C.W.Zhang, Q.Gao, J.Huang, W.Wang. *J. Am. Chem. Soc.*, **135**, 13567 (2013); https://doi.org/10.1021/ja406978q
228. A.Oda, H.Torigoe, A.Itadani, T.Ohkubo, T.Yumura, H.Kobayashi, Y.Kuroda. *J. Phys. Chem. C*, **117**, 19525 (2013); https://doi.org/10.1021/jp4065517
229. A.A.Gabrienko, S.S.Arzumanov, M.V.Luzgin, A.G.Stepanov, V.N.Parmon. *J. Phys. Chem. C*, **119**, 24910 (2015); https://doi.org/10.1021/acs.jpcc.5b08759
230. A.G.Stepanov, S.S.Arzumanov, A.A.Gabrienko. *Chem.: Methods*, **1**, 224 (2021); https://doi.org/10.1002/cmtd.202100021
231. M.H.Mahyuddin, S.Tanaka, Y.Shiota, K.Yoshizawa. *Bull. Chem. Soc. Jpn.*, **93**, 345 (2020); https://doi.org/10.1246/bcsj.20190282
232. P.Zhang, X.Yang, X.Hou, J.Mi, Zh.Yuan, J.Huang, C.Stampfl. *Catal. Sci. Technol.*, **9**, 6297 (2019); https://doi.org/10.1039/C9CY01749F
233. S.S.Arzumanov, A.A.Gabrienko, D.Freude, A.G.Stepanov. *Catal. Sci. Technol.*, **6**, 6381 (2016); https://doi.org/10.1039/C6CY00878J
234. A.A.Kolganov, A.A.Gabrienko, I.Yu.Chernyshov, A.G.Stepanov, E.A.Pidko. *Phys. Chem. Chem. Phys.*, **24**, 6492 (2022); https://doi.org/10.1039/D1CP05854A
235. D.Soulivong, S.Norsic, M.Taoufik, C.Coperet, J.Thivolle-Cazat, S.Chakka, J.M.Basset. *J. Am. Chem. Soc.*, **130**, 5044 (2008); https://doi.org/10.1021/ja800863x
236. Y.Meng, C.Ding, X.Gao, L.Ma, K.Zhang, J.Wang, Z.Li. *Appl. Surf. Sci.*, **513**, 145724 (2020); https://doi.org/10.1016/j.apsusc.2020.145724
237. M.Bhati, J.Dhumal, K.Joshi. *New J. Chem.*, **46**, 70 (2022); https://doi.org/10.1039/D1NJ04525C
238. Y.Meng, C.Ding, Y.Xue, X.Gao, K.Zhang, J.Wang, Z.Li. *New J. Chem.*, **44**, 3922 (2020); https://doi.org/10.1039/C9NJ04723A
239. Y.Turap, I.Wang, T.Fu, Y.Wu, Y.Wang, W.Wang. *Int. J. Hydrogen Energy*, **45**, 6538 (2020); https://doi.org/10.1016/j.ijhydene.2019.12.223
240. P.Mousavian, M.D.Esrafili, J.J.Sardroodi. *New J. Chem.*, **45**, 19842 (2021); https://doi.org/10.1039/D1NJ03456A
241. J.Y.Yuan, W.H.Zhang, X.X.Li, J.L.Yang. *Chem. Commun.*, **54**, 2284 (2018); https://doi.org/10.1039/C7CC08713F
242. N.Pantha, K.Ulman, S.Narasimhan. *J. Chem. Phys.*, **153**, 244701 (2020); https://doi.org/10.1063/5.0035353
243. S.Zhang, X.Lv, J.Wang, T.Wang, J.Shan. *J. Mol. Model.*, **27**, 346 (2021); https://doi.org/10.1007/s00894-021-04971-2
244. Y.J.Xi, A.Heyden. *ACS Catal.*, **9**, 6073 (2019); https://doi.org/10.1021/acscatal.9b01619
245. H.T.Zhang, C.Liu, P.Liu, Y.H.Hu. *J. Chem. Phys.*, **151**, 024304 (2019); https://doi.org/10.1063/1.5110875

246. D.Seeburg, D.Liu, R.Dragomirova, H.Atia, M.M.Pohl, H.Amani, G.Georgi, S.Kreft, S.Wohlrab. *Processes*, **6**, 263 (2018); https://doi.org/10.3390/pr6120263
247. L.Chen, Zh.Qi, Sh.Zhang, J.Su, G.A.Somorjai. *Catalysts*, **10**, 858 (2020); https://doi.org/10.3390/catal10080858
248. X.L.Yin, L.H.Shen, S.Wang, B.Y.Wang, C.Shen. *Appl. Catal. B*, **301**, 120816 (2022); https://doi.org/10.1016/j.apcatb.2021.120816
249. D.Sheldon. *Johnson Matthey Technol. Rev.*, **61**, 172 (2017); https://doi.org/10.1595/205651317X695622
250. G.Bozzano, F.Manenti. *Prog. Energy Combust. Sci.*, **56**, 71 (2016); https://doi.org/10.1016/j.pecs.2016.06.001
251. H.T.Luk, C.Mondelli, D.C.Ferre, J.A.Stewart, J.Perez Ramirez. *Chem. Soc. Rev*, **46**, 1358 (2017); https://doi.org/10.1039/C6CS00324A
252. E.Y.Asalieva, E.V.Kul'chakovskaya, L.V.Sineva, V.Z.Mordkovich. *Petrol. Chem.*, **60**, 69 (2020); https://doi.org/10.1134/S0965544120010028
253. A.C.Chien, B.Y. Liao. *RSC Adv.*, **10**, 26693 (2020); https://doi.org/10.1039/D0RA02051F
254. I.V.Zagaynov, A.S.Loktev, I.E.Mukhin, A.G.Dedov, I.I.Moiseev. *Mendeleev Commun.*, **27**, 509 (2017); https://doi.org/10.1016/j.mencom.2017.09.027
255. M.Li, Zh.Sun,Y.H.Hu. *J. Mater. Chem. A*, **9**, 12495 (2021); https://doi.org/10.1039/D1TA00440A
256. J.W.Han, J.S.Park, M.S.Choi, H.Lee. *Appl. Catal. B*, **203**, 625 (2017); https://doi.org/10.1016/j.apcatb.2016.10.069
257. R.B.Duarte, F.Krumeich, J.A.Van Bokhoven. *ACS Catal.*, **4**, 1279 (2014); https://doi.org/10.1021/cs400979q
258. Y.Hou, Sh.Ogasawara, A.Fukuoka, H.Kobayashi. *Catal. Sci. Technol.*, **7**, 6132 (2017); https://doi.org/10.1039/C7CY02183F
259. Y.Chen, B.deGlee, Y.Tang, Z.Wang, B.Zhao, Y.Wei, L.Zhang, S.Yoo, K.Pei, J.H.Kim, Y.Ding, P.Hu, F.F.Tao, M.Liu. *Nat. Energy*, **3**, 1042 (2018); https://doi.org/10.1038/s41560-018-0262-5
260. K.B.Golubev, O.V.Yashina, T.I.Batova, N.V.Kolesnichenko, N.N.Ezhova. *Petrol. Chem.*, **61**, 663 (2021); https://doi.org/10.1134/S0965544121040058
261. E.G.Chepaikin, A.P.Bezruchenko, G.N.Boiko, A.E.Gekhman, I.I.Moiseev. *Kinet. Catal.*, **47**, 12 (2006); https://doi.org/10.1134/S0023158406010034
262. H.Zhou, T.Y.Liu, X.Y.Zhao, Y.F.Zhao, H.Lv, S.Fang, X.Q.Wang, F.Y.Zhou, Q.Xu, J.Xu, C.Xiong, Z.G.Xue, K.Wang, W.C.Cheong, W.Xi, L.Gu, T.Yao, S.Q.Wei, X.Hong, J.Luo, Y.F.Li, Y.E.Wu. *Angew. Chem., Int. Ed.*, **58**, 18388 (2019); https://doi.org/10.1002/anie.201912785
263. Y.Tang, Y.Li, V.Fung, D.Jiang, W.Huang, Sh.Zhang, Y.Iwasawa, T.Sakata, L.Nguyen, X.Zhang, A.I.Frenkel, F.Tao. *Nat. Commun.*, **9**, 1231 (2018); https://doi.org/10.1038/s41467-018-03235-7
264. B.Wu, R.O.Yang, L.Shi, T.J.Lin, X.Yu, M.Huang, K.Gong, F.F.Sun, Z.Jiang, S.G.Li, L.S.Zhong, Y.H.Sun. *Chem. Commun.*, **56**, 14677 (2020); https://doi.org/10.1039/D0CC06492K
265. Q.Zhao, B.Liu, Y.B.Xu, F.Jiang, X.H.Liu. *New J. Chem.*, **44**, 1632 (2020); https://doi.org/10.1039/c9nj05667j
266. C.Kalamaras, D.Palomas, R.Bos, A.Horton, M.Crimmin, K.Hellgardt. *Catal. Lett.*, **146**, 483 (2016); https://doi.org/10.1007/s10562-015-1664-7
267. C.Hammond, M.M.Forde, M.H.Ab-Rahim, A.Thetford, Q.He, R.L.Jenkins, N.Dimitratos, J.A.Lopez-Sanchez, N.F.Dummer, D.M.Murphy, A.F.Carley, S.H.Taylor, D.J.Willock, E.E.Stangland, J.Kang, H.Hagen, C.J.Kiely, G.J.Hutchings. *Angew. Chem., Int. Ed.*, **51**, 5129 (2012); https://doi.org/10.1002/anie.201108706
268. O.P.Taran, S.A.Yashnik, V.V.Boltenkov, E.V.Parkhomchuk, K.A.Sashkina, A.B.Ayusheev, D.E.Babushkin, V.N.Parmon. *Top. Catal.*, **62**, 491 (2019); https://doi.org/10.1007/s11244-019-01151-8
269. B.Wu, T.Lin, Zh.Lu, X.Yu, M.Huang, R.Yang, C.Wang, Ch.Tian, J.Li, Y.Sun, L.Zhong. *Chem.*, **8**, 1658 (2022); https://doi.org/10.1016/j.chempr.2022.02.001
270. X.Sun, Y.J.Gao, C.X.Zhao, S.W.Deng, X.Zhong, G.L.Zhuang, Z.Z.Wei, J.G.Wang. *Adv. Theory Simul.*, **2**, 1800158 (2019); https://doi.org/10.1002/adts.201800158
271. T.Moteki, N.Tominaga, M.Ogura. *ChemCatChem.*, **12**, 2957 (2020); https://doi.org/10.1002/cctc.202000168
272. N.V.Kolesnichenko, Y.M.Snatenkova, T.I.Batova, O.V.Yashina, K.B.Golubev. *Micropor. Mesopor. Mater.*, **330**, 111581 (2022); https://doi.org/10.1016/j.micromeso.2021.111581
273. N.V.Kolesnichenko, T.I.Batova, A.N.Stashenko, T.K.Obukhova, E.V.Khramov, A.A.Sadovnikov, D.E.Zavelev. *Micropor. Mesopor. Mater.*, **344**, 112239 (2022); https://doi.org/10.1016/j.micromeso.2022.112239
274. J.D.Kistler, N.Chotigkrai, P.Xu, B.Enderle, P.Praserthdam, C.Y.Chen, N.D.Browning, B.C.Gates. *Angew. Chem., Int. Ed.*, **53**, 8904 (2014); https://doi.org/10.1002/anie.201403353
275. J.Lu, C.Aydin, N.D.Browning, B.C.Gates. *Angew. Chem., Int. Ed.*, **51**, 5842 (2012); https://doi.org/10.1002/anie.201107391
276. W.Shang, M.Gao, Y.Chai, G.Wu, N.Guan, L.Li. *ACS Catal.*, **11**, 7249 (2021); https://doi.org/10.1021/acscatal.1c00950
277. K.Narsimhan, V.K.Michaelis, G.Mathies, W.R.Gunther, R.G.Griffin, Y.Román-Leshkov. *J. Am. Chem. Soc.*, **137**, 1825 (2015); https://doi.org/10.1021/ja5106927
278. J.Zhu, V.L.Sushkevich, A.J.Knorpp, M.A.Newton, S.C.M.Mizuno, T.Wakihara, T.Okubo, Z.D.Liu, J.A.VanBokhoven. *Chem. Mater.*, **32**, 1448 (2020); https://doi.org/10.1021/acs.chemmater.9b04223
279. C.X.Zhou, H.L.Zhang, L.F.Yang, D.F.Wu, S.He, H.C.Yang, H.F.Xiong. *Fuel*, **309**, 122178 (2022); https://doi.org/10.1016/j.fuel.2021.122178
280. A.Abedin, J.J.Spivey. In *Advances in Sustainable Energy: Direct Catalytic Low-temperature Conversion of CO_2 and Methane to Oxygenates*. (Eds Y.Gao, W.Song, J.L.Liu, S.Bashir). (Cham: Springer, 2021). P. 227; https://doi.org/10.1007/978-3-030-74406-9_8
281. E.N.Al-Shafei, M.Z.Albahar, M.F.Aljishi, H.H.Al-Badairy. *Mol. Catal.*, **515**, 111942 (2021); https://doi.org/10.1016/j.mcat.2021.111942
282. N.Kosinov, F.J.A.G.Coumans, E.A.Uslamin, A.S.G.Wijpkema, B.Mezari, E.J.M.Hensen. *ACS Catal.*, **7**, 520 (2017); https://doi.org/10.1021/acscatal.6b02497
283. I.Julian, M.B.Roedern, J.L.Hueso, S.Irusta, A.K.Baden, R.Mallada, Z.Davis, J.Santamaria. *Appl. Catal. B*, **263**, 118360 (2020); https://doi.org/10.1016/j.apcatb.2019.118360
284. N.K.Razdan, A.Kumar, B.L.Foley, A.Bhan. *J. Catal.*, **381**, 261 (2020); https://doi.org/10.1016/j.jcat.2019.11.004
285. P.F.Xie, T.C.Pu, A.M.Nie, S.Hwang, S.C.Purdy, W.J.Yu, D.Su, J.T.Miller, C.Wang. *ACS Catal.*, **8**, 4044 (2018); https://doi.org/10.1021/acscatal.8b00004
286. N.Kosinov, A.S.G.Wijpkema, E.Uslamin, R.Rohling, F.J.A.G.Coumans, B.Mezari, A.Parastaev, A.S.Poryvaev, M.V.Fedin, E.A.Pidko, E.J.M.Hensen. *Angew. Chem., Int. Ed.*, **57**, 1016 (2018); https://doi.org/10.1002/anie.201711098
287. A.A.Stepanov, L.L.Korobitsyna, A.V.Vosmerikov, V.I.Zaikovskii. *Petrol. Chem.*, **59**, 91 (2019); https://doi.org/10.1134/S0965544119010146
288. A.López-Martín, M.F.Sini, M.G.Cutrufello, A.Caballero, G.Colón. *Appl. Catal. B*, **304**, 120960 (2022); https://doi.org/10.1016/j.apcatb.2021.120960
289. A.Sridhar, M.Rahman, Sh.J.Khatib. *ChemCatChem.*, **10**, 2571 (2018); https://doi.org/10.1002/cctc.201800002
290. V.Abdelsayed, D.Shekhawat, M.W.Smith. *Fuel*, **139**, 401 (2015); https://doi.org/10.1016/j.fuel.2014.08.064
291. T.E.Tshabalala, N.J.Coville, J.A.Anderson, M.S.Scurrell. *Appl. Petrochem. Res.*, **11**, 235 (2021); https://doi.org/10.1007/s13203-021-00274-y

292. Y.Xiao, A.Varma. *ACS Catal.*, **8**, 2735 (2018); https://doi.org/10.1021/acscatal.8b00156
293. X.Guo, G.Fang, G.Li, H.Ma, H.Fan, L.Yu, C.Ma, X.Wu, D.Deng, M.Wei, D.Tan, R.Si, S.Zhang, J.Li, L.Sun, Z.Tang, X.Pan, X.Bao. *Science*, **344**, 616 (2014); https://doi.org/10.1126/science.1253150
294. R.Kojima, S.Kikuchi, H.Ma, J.Bai, M.Ichikawa. *Catal. Lett.*, **110**, 15 (2006); https://doi.org/10.1007/s10562-006-0087-x
295. Y.Liu, F.Kooli, A.Borgna. *Catal. Today*, **357**, 392 (2020); https://doi.org/10.1016/j.cattod.2019.09.026
296. M.Chen, Y.Song, B.Liu, X.Liu, Y.Xu, Zh.G.Zhang. *Fuel*, **262**, 116674 (2020); https://doi.org/10.1016/j.fuel.2019.116674
297. A.López-Martín, A.Caballero, G.Colón. *Mol. Catal.*, **486**, 110787 (2020); https://doi.org/10.1016/j.mcat.2020.110787
298. H.Sheng, E.P.Schreiner, W.Zheng, R.F.Lobo. *ChemPhysChem.*, **19**, 504 (2018); https://doi.org/10.1002/cphc.201701001
299. D.B.Lukyanov, T.J.Vazhnova. *Mol. Catal.*, **342** – **343**, 1 (2011); https://doi.org/10.1016/j.molcata.2011.04.011
300. S.Y.He, T.H.Li, Z.Q.Huang, Y.Liu, J.Li, C.R.Chang. *J. Chem. Phys.*, **154**, 174706 (2021); https://doi.org/10.1063/5.0048962
301. M.Sakbodin, Y.Q.Wu, S.C.Oh, E.D.Wachsman, D.X.Liu. *Angew. Chem., Int. Ed.*, **55**, 16149 (2016); https://doi.org/10.1002/anie.201609991
302. J.Hao, P.Schwach, L.Li, X.Guo, J.Weng, H.Zhang, H.Shen, G.Fang, X.Huang, X.Pan, Ch.Xiao, X.Yang, X.Bao. *J. Energy Chem.*, **52**, 372 (2021); https://doi.org/10.1016/j.jechem.2020.04.001
303. J.Q.Hao, P.Schwach, G.Z.Fang, X.G.Guo, H.L.Zhang, H.Shen, X.Huang, D.Eggart, X.L.Pan, X.H.Bao. *ACS Catal.*, **9**, 9045 (2019); https://doi.org/10.1021/acscatal.9b01771
304. A.Puente-Urbina, Z.Pan, V.Paunović, P.Šot, P.Hemberger, J.A.Van Bokhoven. *Angew. Chem., Int. Ed.*, **60**, 24002 (2021); https://doi.org/10.1002/anie.202107553
305. R.S.Postma, L.Lefferts. *React. Chem. Eng.*, **6**, 2425 (2021); https://doi.org/10.1039/D1RE00261A
306. H.E.Toraman, K.Alexopoulos, S.Ch.Oh, S.Cheng, D.Liu, D.G.Vlachos. *Chem. Eng. J.*, **420**, 130493 (2021); https://doi.org/10.1016/j.cej.2021.130493
307. J.Xiong, H.Yu, Y.Wei, Ch.Xie, K.Lai, Zh.Zhao, J.Liu. *Catalysts*, **12**, 713 (2022); https://doi.org/10.3390/catal12070713